

**In compliance with the
Canadian Privacy Legislation
some supporting forms
may have been removed from
this dissertation.**

**While these forms may be included
in the document page count,
their removal does not represent
any loss of content from the dissertation.**

The Influence of Ionic Strength and Fluoride Ion Concentration on the
Adsorption Properties of Gibbsite: Phosphate and Arsenate Adsorption

by

Alain Garand

November, 2002

A thesis submitted to the Graduate and Postgraduate Studies Office in partial
fulfillment of the requirements of the degree of Master of Science.

Department of Earth and Planetary Sciences

McGill University

3450 University St.

Montreal, Quebec, Canada

H3A 2A7

Alain Garand © 2002



National Library
of Canada

Bibliothèque nationale
du Canada

Acquisitions and
Bibliographic Services

Acquisisitons et
services bibliographiques

395 Wellington Street
Ottawa ON K1A 0N4
Canada

395, rue Wellington
Ottawa ON K1A 0N4
Canada

Your file *Votre référence*
ISBN: 0-612-88198-9
Our file *Notre référence*
ISBN: 0-612-88198-9

The author has granted a non-exclusive licence allowing the National Library of Canada to reproduce, loan, distribute or sell copies of this thesis in microform, paper or electronic formats.

L'auteur a accordé une licence non exclusive permettant à la Bibliothèque nationale du Canada de reproduire, prêter, distribuer ou vendre des copies de cette thèse sous la forme de microfiche/film, de reproduction sur papier ou sur format électronique.

The author retains ownership of the copyright in this thesis. Neither the thesis nor substantial extracts from it may be printed or otherwise reproduced without the author's permission.

L'auteur conserve la propriété du droit d'auteur qui protège cette thèse. Ni la thèse ni des extraits substantiels de celle-ci ne doivent être imprimés ou autrement reproduits sans son autorisation.

Canada

Abstract

Anomalously high concentrations of arsenic and phosphate are found in the sediments of the Saguenay Fjord relative to those of the Gulf and St. Lawrence Estuary. Whereas the source of phosphate is likely anthropogenic, arsenic appears to be scavenged from the bottom marine waters by settling detrital and authigenic particles. The surface waters of the Saguenay Fjord show a particulate aluminum anomaly ($[Al]_{tot}/[Al]_{diss} > 1$) that decreases downstream or with increasing salinity. The mineralogy of the aluminum particulate matter may be akin to gibbsite given the refining activities in the region. The adsorption of phosphate and arsenic to various mineral oxides is well established but the scavenging capacity of gibbsite in this estuarine environment is not known. -

In order to simulate the behavior of the adsorbent/adsorbate relationship during estuarine mixing, the adsorption capacity of gibbsite for arsenate and phosphate was measured in pure water; 0.67 M NaCl; 10 mM CaCl₂; 10 mM CaCl₂ + 0.64 M NaCl and in seawater in the absence and presence of the fluoride ion. Particular attention was paid to the fluoride ion because of its status as a major seawater constituent and its known affinity for the gibbsite surface.

In the absence of the fluoride ion, adsorption of both arsenate and phosphate decreases with increasing ionic strength. The presence of Ca partially offsets the decreased adsorption with ionic strength but the presence of other seawater constituents partially counteracts its effect. The increase in adsorption in the presence of Ca is attributed to the formation of ternary surface complexes between Ca, phosphate or arsenate, and the gibbsite surface.

In the presence of the fluoride ion, arsenate adsorption increases in all experimental solutions compared to pure water whereas the adsorption of phosphate decreases relative to pure water. The differential adsorption behavior of the two adsorbates is attributed to the formation of arsenate-fluoride aqueous complexes and their affinity for the gibbsite surface. The absence of a similar behavior with phosphate may reflect a lack of affinity or availability of phosphate-fluoride complexes.

Adsorption experiments carried out in the presence of fluoride were buffered by the addition of fluorite crystals. A search of the literature revealed that published values of the thermodynamic solubility constant, K_{sp}^0 , of fluorite in water are highly variable.

Consequently, the equilibrium activity of the fluoride ion in our experimental solutions could not be estimated accurately. In addition, the ion activity coefficient of the fluoride ion, γ_{F^-} , in seawater was the subject of a single experimental study under conditions that are not truly representative of natural marine systems. Given these uncertainties, we measured the fluorite equilibrium ion concentration products (ICP = $[Ca^{2+}][F^-]^2$) at 25°C and 1 atmosphere total pressure in pure water, 0.1, 0.4 and 0.7 molar NaCl solutions to investigate the effect of ionic strength and in 10 mM $CaCl_2$ + 0.64 M NaCl, 10 mM $CaCl_2$ + 0.484 M NaCl + 52 mM $MgCl_2$ and seawater solutions to determine the influence of some major seawater constituents and possible co-precipitation, on the solubility of fluorite. In the latter solutions, equilibrium was approached from both undersaturation (i.e., initial $[F^-] = 0$) and supersaturation (i.e., initial $[F^-] = 15$ times the seawater value $\cong 1$ mM) to test for reversibility and confirm equilibrium.

The ion concentration products measured after 32 weeks of equilibration become invariant or converge to constant values. The fluorite K_{sp}^0 (or equilibrium ion activity product = IAP = $a_{Ca^{2+}} a_{F^-}^2$) measured in pure water is $3.07 \pm 0.09 * 10^{-11}$ whereas the average value for the pure water, NaCl and Na-Cl-Ca solutions combined is $3.08 \pm 0.08 * 10^{-11}$.

Experiments run in Na-Cl-Ca-Mg and artificial seawater solutions failed to reproduce the K_{sp}^0 obtained in pure water and the simple salt solutions. Part of this discrepancy could be attributed to the inaccuracy of activity coefficient estimates obtained from speciation models, but we believe that they result from the formation of Mg bearing CaF_2 solid solutions on the surface of fluorite. Since the equilibrium ion activity product is more than one order of magnitude larger in the Na-Cl-Ca-Mg solution than in artificial seawater we can only assume that other seawater constituents affect the composition of the solubility-controlling phase, possibly Sr^{2+} , CO_3^{2-} and boric acid.

Résumé

On retrouve des concentrations élevées d'arsenic et de phosphate dans les sédiments du Fjord du Saguenay comparativement aux sédiments du Golfe et de l'Estuaire du St Laurent. Tandis que la source de phosphate est vraisemblablement anthropique, l'arsenic semble être capté des eaux marines profondes par la matière particulaire qui sédimente. Les eaux de surface du Fjord du Saguenay contiennent des fortes concentrations d'aluminium particulaire ($[Al]_{tot}/[Al]_{diss} > 1$) lesquelles diminuent en aval ou avec l'augmentation de la salinité. Une partie de l'aluminium particulaire est probablement constituée de gibbsite, un produit des activités d'affinage dans la région. L'efficacité de l'adsorption du phosphate et de l'arsenic par les oxydes métalliques est bien établie mais la capacité d'adsorption de la gibbsite (hydroxide d'aluminium) dans cet environnement demeure inconnue.

Afin de simuler le comportement de l'adsorbant et des espèces adsorbées durant le mélange estuarien, la capacité d'adsorption de la gibbsite pour le phosphate et l'arsenate a été mesurée dans de l'eau pure et les solutions suivantes: 0.67 M NaCl; 10 mM CaCl₂; 10 mM CaCl₂ + 0.64 M NaCl et dans l'eau de mer, en absence ainsi qu'en présence de l'ion fluorure. Une attention particulière a été portée à l'ion fluorure à cause de son statut d'ion majeur dans l'eau de mer ainsi que de sa forte affinité pour la surface de la gibbsite.

En absence de l'ion fluorure, l'adsorption du phosphate et de l'arsenate diminue avec l'augmentation de la force ionique. La présence de Ca contrebalance partiellement la diminution due à l'augmentation de la force ionique, mais son effet est contré en présence d'autres ions majeurs de l'eau de mer. L'augmentation de l'adsorption en présence de Ca est attribuée à la formation de complexes ternaires entre le Ca, le phosphate ou l'arsenate, et la surface de la gibbsite.

En présence d'ions fluorure, l'adsorption de l'arsenate augmente dans toutes les solutions comparativement à l'eau pure tandis que l'adsorption de phosphate diminue comparativement à l'eau pure. Cette différence de comportement est attribuée à la formation de complexes arsenate-fluorure aqueux et à leurs affinités pour la surface de la

gibbsite. Dans le cas du phosphate, le complexe phosphate-fluorure est soit absent ou possède une très faible affinité pour la surface de la gibbsite.

Dans les expériences en présence de l'ion fluorure, ceux-ci ont été tamponnés par l'addition d'un cristal de fluorite. Une recherche bibliographique a révélé que les valeurs publiées de la constante de solubilité, K_{sp}^0 , de la fluorite sont très variables. Par conséquent, l'activité de l'ion fluorure, F^- , à l'équilibre dans nos solutions expérimentales ne pouvait être évaluée exactement. De plus, la valeur du coefficient d'activité de l'ion fluorure (γ_F) dans l'eau de mer a été évaluée expérimentalement à une seule reprise, et ce, sous des conditions qui ne reflètent pas les conditions naturelles. Nous avons donc entrepris des expériences d'équilibration de la fluorite à 25 °C et 1 atmosphère de pression dans des solutions d'eau pure et dans des solutions de 0.1, 0.4 et 0.7 M NaCl afin de déterminer l'effet de la force ionique, ainsi que dans des solutions de 10 mM CaCl₂ + 0.64 M NaCl, 10 mM CaCl₂ + 0.484 M NaCl + 52 mM MgCl₂ et dans l'eau de mer afin d'étudier l'influence des ions majeurs de l'eau de mer et leur co-précipitation potentielle, sur la solubilité de la fluorite. Dans ces derniers cas, l'équilibre a été approché à partir de solutions sous-saturées ($[F]_{init} = 0$) et sur-saturées ($[F]_{init} = 15$ fois sa concentration dans l'eau de mer $\cong 1$ mM) pour vérifier la réversibilité de la réaction ainsi que confirmer l'équilibre.

Dans l'eau pure ainsi que dans des solutions simples (Na-Cl-Ca), le produit de l'activité des ions à l'équilibre ($PAI = K_{sp}^0 = a_{Ca^{2+}} a_{F^-}^2$) est, en moyenne, égal à $3.06 \pm 0.08 * 10^{-11}$, une valeur identique à une des valeurs rapportées dans la littérature. En contrepartie, le PAI à l'équilibre mesuré dans les solutions de Na-Cl-Ca-Mg et d'eau de mer est respectivement, plus élevé et plus bas que le K_{sp}^0 . Nous proposons qu'une solution-solide de fluorite contenant du Mg mais de composition indéterminée contrôle la solubilité dans ces solutions.

Preface

This thesis consists of 4 chapters. The first chapter is a general introduction to the thesis. The second chapter is in manuscript format, and is intended for submission to the refereed journal *Chemical Geology*. The third chapter is also in manuscript format, and is intended for submission to the refereed journal *Marine Chemistry*. Both manuscripts have been integrated as chapters formatted to the general layout of the thesis. The fourth chapter is the conclusion and includes the contributions to knowledge and suggestions for future work.

The following is excerpted from Guidelines for Thesis Preparation, office of Graduate and Postgraduate Studies, McGill University:

“Candidates have the option of including, as part of the thesis, the text of one or more papers submitted for publication, or the clearly-duplicated text of one or more published papers. These texts must be bound as an integral part of the thesis.

If this option is chosen, connecting texts that provide logical bridges between the different papers are mandatory. The thesis must be written in such a way that is more than a mere collection of manuscripts; in other words, results of a series of papers must be integrated.

The thesis must still conform to all other requirements of the “guidelines for thesis preparation”. The thesis must include: A Table of Contents, an abstract in English and French, an introduction which clearly states the rationale and objectives of the study, a review of literature, a final conclusion and summary, and a thorough bibliography or reference list.

Additional material must be provided where appropriate (e.g. in appendices) and in sufficient detail to allow clear and precise judgment to be made of the importance and originality of the research reported in the thesis.

In the case of manuscripts co-authored by the candidate and others, the candidate is required to make an explicit statement in the thesis as to who contributed to such work and to what extent. Supervisors must attest to the accuracy of such statements at the doctoral defence. Since the task of the examiner is made more difficult in these cases, it is in the candidate’s interest to make perfectly clear the responsibilities of all authors of the co-authored papers.”

Contributions of Authors

The author and Prof. Alfonso Mucci designed the experimental protocols devised to verify the hypotheses put forth in this thesis. The author performed all the experimental and most of the analytical work. The interpretation of the results is solely the responsibility of the author who did benefit from critical comments and suggestions from Prof. Mucci.

Funding for this project was provided by the Natural Sciences and Engineering Research Council of Canada (NSERC) strategic (#201981-97) and research grants to Prof. Mucci. Financial support to the author was provided by Les Fonds pour la Formation des Chercheurs et l'Aide à la Recherche du Québec (FCAR) in the form of a post-graduate scholarship. Additional funding to the author was provided by the Department of Earth and Planetary Sciences at McGill University in the form of scholarships, teaching and research assistantships.

Acknowledgements

I would like to express my sincere gratitude to Dr. Al Mucci for letting me work with him on this project. It was a wonderful learning experience and your guidance was invaluable. Thank you for your enthusiasm, patience, friendship and time.

I must also thank C. Guignard for her friendship and providing critical help in the laboratory and solving an infinite number of problems; S.K.Sears for help with the XRD and providing the SEM scans; G. Keating and S. Lalli for their technical support with the use of AAS, XRD and XRF; G. Panagiotidis for any and all tools and technical assistance; B.Dionne for computer assistance; Prof. R. Martin for his fountain of references; A. Kosowski and C. Mathews for great laughs and solving any administrative issues; S. Archibald, A. Migdisov and D. Dolejs for theoretical discussions and computer assistance; S.Musclow, K. Bibeau and R. Nelson for laboratory help, and Prof. F. Millero for answering numerous questions and providing the Pitzer Model Excel Macro.

Thank you B. Kennedy, S. Modeland, K. Ault, C. Mann, M. Richer, Y. Lavallee, A. Villegas, A. Chouinard, S.T. Kim, J. Chien, G. Bernier, S. Rahman, the crew of the Alcide C. Horth and anyone else who I may have forgotten for the great times. I would like to thank my family and a very special thanks goes out to the fabulous and greatest love of mine Meredith Willis and Dr. Sinclair and the staff at the Montreal Neurological Institute for saving our lives.

Table of Contents

Abstract	ii
Resume	iv
Preface	vi
Contributions of Authors	vii
Acknowledgements	viii
Table of Contents	ix
List of Figures	xi
List of Tables	xii
CHAPTER 1: GENERAL INTRODUCTION	1
1.1 Arsenic in the Saguenay Fjord	3
1.2 Phosphorus in the Saguenay Fjord	5
1.3 Particulate Aluminum in the Saguenay Fjord	7
1.4 Adsorption of Arsenate and Phosphate	10
1.5 Adsorption in the Presence of Seawater Constituents	12
1.6 Objectives	14
1.7 References	17
CHAPTER 2: THE INFLUENCE OF IONIC STRENGTH AND THE FLUORIDE ION CONCENTRATION ON THE ADSORPTION PROPERTIES OF GIBBSITE: PHOSPHATE AND ARSENATE ADSORPTION	26
Forward	27
2.1 Abstract	29
2.2 Introduction	30
2.3 Materials and Methods	36
2.4 Results	42
2.4.1 Arsenate Adsorption in the Absence of Fluoride	44
2.4.2 Arsenate Adsorption in the Presence of Fluoride	47
2.4.3 Phosphate Adsorption in the Absence of Fluoride	49
2.4.4 Phosphate Adsorption in the Presence of Fluoride	51
2.5 Discussion	54
2.5.1 Effect of Ionic Strength on the Adsorption of Arsenate and Phosphate to Gibbsite	54
2.5.2 Effect of Ca at its Seawater Concentration and Speciation on Arsenate and Phosphate Adsorption on Gibbsite in Fluoride-Free Solutions	55
2.5.3 Arsenate and Phosphate Adsorption on Gibbsite in Fluoride-Free Artificial Seawater	57
2.5.4 Effect of the Fluoride Ion on the Adsorption of Arsenate on Gibbsite	58
2.5.5 Effect of the Fluoride Ion on the Adsorption of Phosphate on Gibbsite	59
2.5.6 Comparison Between Arsenate and Phosphate Adsorption	60

2.6	Conclusions	61
2.7	References	64
2.8	Appendix	71
CHAPTER 3: THE INFLUENCE OF IONIC STRENGTH AND SOLUTION COMPOSITION ON THE SOLUBILITY OF FLUORITE AT 25 °C AND ONE ATMOSPHERE TOTAL PRESSURE.		74
	Forward	75
3.1	Abstract	77
3.2	Introduction	78
3.3	Materials and Methods	81
3.4	Results and Discussion	85
3.5	Conclusions	90
3.6	References	91
3.7	Appendix	93
CHAPTER 4: CONCLUSION		95
	Contribution to Knowledge	96
	Suggestions for Future Research	99

List of Figures

1.0	Map of the Saguenay Fjord and Gulf of St. Lawrence, Quebec, Canada.	2
1.1	Sphere model of polymeric $\text{Al}_6(\text{OH})_{12}(\text{H}_2\text{O})_{12}^{6+}$.	8
1.2	Solubility of gibbsite in freshwater and seawater (S= 35) calculated using compilation of Stumm & Morgan (1996).	9
1.3	Activity-activity (predominance) diagram illustrating the field of stability of gibbsite.	10
2.4.1	Adsorption isotherms of arsenate onto gibbsite in F^- free solutions after 15 days @ 23 ± 1 °C and pH 7.20 ± 0.10 .	44
2.4.2	Adsorption isotherms of arsenate onto gibbsite in F^- buffered solutions after 15 days @ 23 ± 1 °C and pH 7.00 ± 0.15 .	47
2.4.3	Adsorption isotherms of phosphate onto gibbsite in F^- free solutions after 15 days @ 23 ± 1 °C and pH 7.12 ± 0.19 .	49
2.4.4	Adsorption isotherms of phosphate onto gibbsite in F^- buffered solutions after 15 days @ 23 ± 1 °C and pH = 7.20 ± 0.18 .	52
3.0	Measured ion concentration products (ICP) for the Na-Cl-Ca, Na-Cl-Ca-Mg and seawater solutions as a function of the period of equilibration.	85
3.1	The stoichiometric solubility constant of fluorite in NaCl solutions of various ionic strengths at 25°C and 1 atmosphere total pressure.	86

List of Tables

2.0	Gibbsite major and trace element composition (XRF).	36
2.1	Fluorite major and trace element composition (XRF).	37
2.4.1	Freundlich and Langmuir parameters of arsenate adsorption isotherms in fluoride-free solutions.	46
2.4.2	Re-calculated K_F values for each type of experimental solution with an average β of 0.6.	46
2.4.3	Freundlich parameters of arsenate adsorption isotherms in the fluoride-buffered solutions.	48
2.4.4	Re-calculated K_F values for each type of experimental solution with an average β of 1.3.	48
2.4.5	Freundlich parameters of phosphate adsorption isotherms in the fluoride-free solutions.	50
2.4.6	Re-calculated K_F values for each type of experimental solution with an average β of 0.44.	51
2.4.7	Freundlich parameters of phosphate adsorption isotherms in the fluoride-buffered solutions.	53
3.0	Compilation of fluorite K_{sp}^0 values reported in the literature.	79
3.1	Fluorite major and trace element composition (XRF).	81
3.2	Results of the 32 and 64-week pure water, NaCl, Na-Cl-Ca and seawater solution sample analyses and the 20 and 24 week Na-Cl-Ca-Mg solution sample analyses.	86

CHAPTER 1

General Introduction

In recent years the waters and sediments of the Saguenay Fjord have been the object of intense research activity. The research has revealed peculiar geochemical anomalies including elevated levels of iron monosulfides (Mucci and Edenborn, 1992; Gagnon et al., 1995), trace metals (Loring and Bowers, 1978; Barbeau et al., 1981; Loring et al., 1983; Pelletier and Canuel, 1988; Cossa, 1990; Gagnon et al., 1993, 1997), arsenic and phosphate in the sediments (Belzile and Lebel, 1986; Richard, 1997; Ouellet, 1979; Primeau and Goulet, 1983; Mucci et al., 2000) as well as elevated levels of particulate aluminum in the water column of the Fjord (S. Alpay, pers. comm).

The Saguenay Fjord, the largest fjord in eastern Canada, is a long and narrow glacially-scoured submerged U-shaped valley which joins the St-Lawrence Estuary at Tadoussac (Figure 1.0). Two shallow sills subdivide the Fjord into two distinct basins, the largest of which, the “interior basin”, extends from the sill westward to the Baie des Ha!Ha! reaching a maximum depth of 275 m (Mucci et al., 2000).

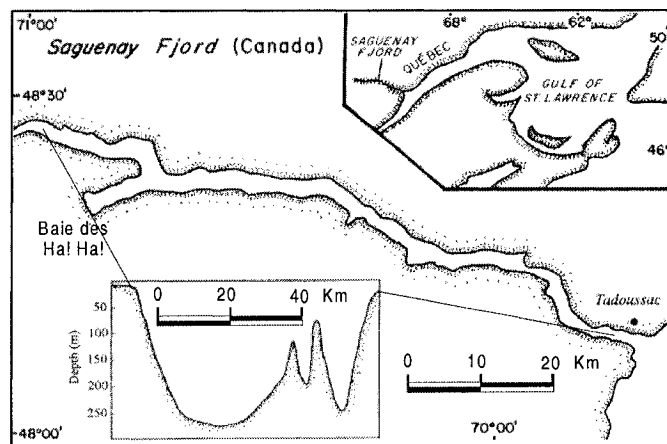


Figure 1.0 Map of the Saguenay Fjord and Gulf of St. Lawrence, Quebec, Canada.

The water column of the Fjord is characterized by a thin freshwater lens, a strong near-surface (10-15m) halocline, and well mixed marine waters below 30 m. These bottom waters, originating from the St. Lawrence Estuary (Therriault and Lacroix, 1975; Seibert et al., 1979), have a salinity of about 30, are well oxygenated and display only minor annual temperature variations; -1 to 1 °C (Drainville, 1968; Sundby and Loring, 1978; Gratton, 1995)

The watershed of the Saguenay Fjord is heavily industrialized and includes aluminum smelters and refineries; paper mills; and a niobium mine and also supports a strong agricultural sector. Historically unregulated, these activities have been responsible for elevated levels of Hg and a variety of polycyclic aromatic hydrocarbons in both the waters and sediments of the Fjord (Fortin and Pelletier, 1995). On the other hand, Mucci et al. (2000) showed that elevated levels of As and P in the sediments are the result of efficient scavenging by suspended particulate matter (SPM) as it settles through the marine waters of the Fjord and are not entirely of anthropogenic origin.

1.1 Arsenic in the Saguenay Fjord

Despite potential As contamination by bauxite discharged at Baie des Ha! Ha! and lost during its unloading (J. Labrie pers. comm.) as well as drainage from a niobium mine, dissolved arsenic concentrations in the waters of the river and the freshwater lens of the Fjord are amongst the lowest (1.1 to 18.7 nM over the salinity range of 0-31) reported for industrialized and “pristine” estuaries (Primeau and Goulet, 1983; Tremblay and Gobeil, 1990; Mucci et al., 2000). Nevertheless, the surface sediments of the Fjord display a strong As enrichment (60 ppm) relative to those of the St. Lawrence Estuary (15 ppm) (Mucci et al., 2000). It has been proposed (Tremblay and Gobeil, 1990; Mucci et

al., 2000) that the arsenic that accumulates at the sediment surface originates from scavenging by detrital and authigenic particles as they settle through the marine water column.

North Atlantic intermediate waters feed the St. Lawrence Estuary and carry an average arsenic concentration of 26 nM or an As/Cl molar ratio of $\sim 5 \times 10^{-8}$ (Mucci et al., 2000). The cold, intermediate St. Lawrence Estuary waters that spill into the Fjord have a salinity of about 30 and contain 16 nM of arsenic (Tremblay and Gobeil, 1990). Large suspended particulate matter (SPM) concentrations near the sharp halocline of the Fjord (e.g., 4.03 mg/l at 15 m depth; Mucci et al., 2000) form by agglomeration and coagulation as a result of mixing of the river water with seawater and the sharp increase in ionic strength. This SPM is temporarily trapped by the sharp density gradient (Sholkovitz, 1976, 1978; Farley and Morel, 1986; Kraepiel et al., 1997). The SPM is rich in authigenic iron oxides (Mucci et al., 2000) but may also contain some bauxite and gibbsite from the aluminum refining activities. Aluminum has been detected in the SPM by FEG-SEM/EDX, grains show aluminum associated with oxygen suggesting the presence of gibbsite (Mucci and Edenborn, 1992). Ferric oxides and hydroxides (Sadiq, 1990; Morse, 1994), manganese oxides, aluminum hydroxides and organic material are known scavengers of arsenic in estuarine environments (e.g., Smedley and Kinniburgh, 2002). The SPM of the Fjord may have a greater scavenging efficiency for arsenic than the material in the Estuary due to differences in its composition and the presence of a sharp halocline in the water column.

Arsenic is released into aquatic and terrestrial environments from both natural and anthropogenic sources and can be removed from solution by biotic uptake, adsorption,

and precipitation. Thermodynamic calculations (Abdullah et al., 1995; Riedel, 1993; Sadiq, 1992) and field observations confirm that the inorganic arsenate ion, As(V), is the dominant species in oxygenated waters although lesser concentrations of arsenite, As(III) and methylated arsenicals have also been reported (Andreae, 1978; Waslenchuk, 1978; Sanders and Windom, 1980; Sanders, 1983; Seyler and Martin, 1990; Anderson and Bruland, 1991). Arsenate is often taken in lieu of phosphate by aquatic organisms, particularly in phosphate deprived environments, leading to an inhibition of oxidative phosphorylation and growth (NRCC, 1978; Planas and Healy, 1978; Stryer, 1988). Toxicity is highest for the reduced (As(III)) species of arsenic and less so for As (V) and organic arsenicals (Fowler et al., 1979) and manifests itself in humans who have been exposed to arsenic contaminated drinking water through lung and skin cancer, hyperpigmentation, keratosis and vascular disorders (Fowler et al., 1979).

The arsenic cycle is complex (Lantzy and Mackenzie, 1994) and its ultimate sink is ocean sediment through adsorption to and slow absorption within authigenic iron and manganese oxy-hydroxides that accumulate at or above the oxic-suboxic boundary (Sullivan and Aller, 1996). Precipitation in most sedimentary environments is insignificant except under anoxic conditions where reduced sulfur limits arsenic solubility (Widerlund and Ingri, 1995; Smedley and Kinniburgh, 2002). In most sedimentary environments, where reactive Fe is abundant, arsenic will co-precipitate with acid volatile sulfides (AVS) and pyrite (Boyle and Jonasson, 1973; Belzile and Lebel, 1986; Saulnier and Mucci, 2000).

1.2 Phosphorus in the Saguenay Fjord

Phosphorus is an essential nutrient to photosynthetic plants. At high concentrations it is often considered a contaminant since it promotes excessive plant

growth in freshwater. The decay of the plant material and the concomitant depletion of dissolved oxygen leads to eutrophication (Gomez et al., 1999). Sediments receive organic and inorganic phosphorus compounds from the overlying water and surrounding land mass (Sundby et al., 1992). The major anthropogenic source of phosphorus to the Saguenay Fjord is the leaching of fertilizers applied to agricultural plots along the drainage basin. Phosphorus levels in the surface sediments of the Fjord (0.15%) are elevated relative to those of the St. Lawrence Estuary (0.11%) (Mucci et al., 2000). The difference cannot be attributed to differences in the water column concentrations because the phosphate level in the marine waters of the Fjord ($0.2 \mu\text{M}$) is less than in the St. Lawrence Estuary ($0.8 \mu\text{M}$) (Mucci et al., 2000). A greater scavenging efficiency of phosphate by SPM in the Fjord has also been proposed to explain the higher surface sediment concentrations (Lucotte and d'Anglejan, 1988; Mucci et al., 2000). Arsenic and phosphate are both group V elements and thus share similar chemical properties and display similar geochemical behaviors which suggests a similar scavenging process.

The only stable redox state of phosphorus in aqueous solutions is +V, thus inorganic phosphorus is always present as orthophosphate. Phosphorus is removed from solution by precipitation, biotic uptake, and adsorption. The ultimate fate of phosphorus is ocean sediment through adsorption to and slow absorption within authigenic iron oxyhydroxides that accumulate at or above the oxic-suboxic boundary and the precipitation of apatite (Sundby et al., 1992), but the major nutrient status of phosphorus is indicative of the complexity of the phosphorus cycle (Sundby et al., 1992).

1.3 Particulate Aluminum in the Saguenay Fjord

Particulate aluminum concentrations of up to 150 ppb have been measured in the freshwater lens of the Saguenay Fjord (Sundby and Loring, 1978). More recent analyses (i.e. 1996) show that levels have fallen to a maximum of 100 ppb (S. Alpay, pers. comm.). The amount of particulate aluminum in the freshwater lens decreases with distance from the Saguenay River, thus, this trend is indicative of an anthropogenic source. A minor amount may come from erosion and weathering products of exposed bedrock and glacial deposits. Aluminum-rich particles isolated from the SPM were detected by field emission gun-scanning electron microscopy in combination with energy dispersive x-ray analysis (FEG-SEM/EDX). The Al signal is associated with oxygen suggesting the presence of gibbsite (S. Alpay, pers. comm.). The presence of gibbsite in the Fjord sediments was also confirmed by x-ray diffraction (XRD) following a concentration of the clay fraction (S. Alpay, pers. comm.). Gibbsite may enter the Fjord during unloading of bauxite at Baie des Ha! Ha! which is then transported by rail to the various aluminum refining facilities in the region. The production practices of Alcan's refining facilities dictate that the dominant phase of particulate aluminum entering the Fjord from those facilities will be either gibbsite or γ -alumina.

Gibbsite [α -Al(OH)₃] is the most common of the hydrated aluminum oxide minerals. It is a monoclinic mineral that typically forms tabular pseudo-hexagonal crystals. The larger OH ions are arranged in a close-packed double layer structure with the smaller Al³⁺ ions occupying the interstices between the two layers. There is a clear distinction between the basal plane and "edge" planes in the gibbsite structure. The "edge" planes are believed to contain the only adsorption sites on gibbsite (Parfitt et al.,

1977; Russell et al., 1974), whereas the basal surface, although accounting for the majority of the surface area, is inert with respect to adsorption. A detailed description of the gibbsite structure can be found elsewhere (Goldberg et al., 1996).

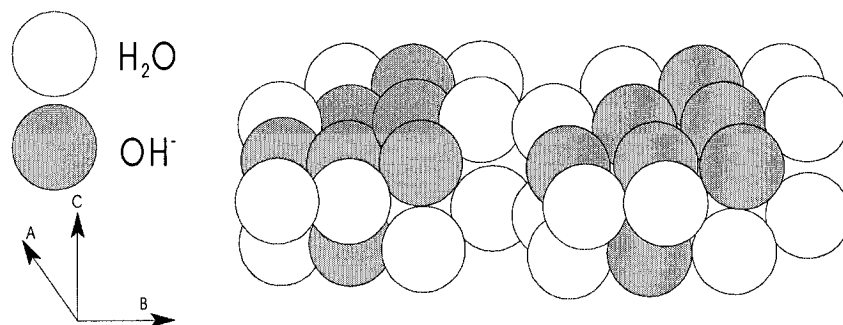
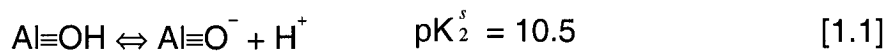


Figure 1.1 Sphere model of polymeric $\text{Al}_6(\text{OH})_{12}(\text{H}_2\text{O})_{12}^{6+}$. Two complete polymeric ions are represented. (After Goldberg et al., 1996)

The hydroxyls on the edge planes are coordinated to a single Al^{3+} ion and the excess charge retains water molecules (Figure 1.1). An adsorbed hydroxyl group replaces the bound water molecule (Goldberg et al., 1996) resulting in an aluminol surface complex ($\text{Al}\equiv\text{OH}$). The protonation and deprotonation of the complex can be described by reactions 1.0 and 1.1 (Manning and Goldberg, 1996) where pK^s represent the intrinsic equilibrium surface constants generated by the constant capacitance model (Stumm and Morgan, 1996).



Other common aluminum minerals are gamma and alpha alumina (corundum) ($\gamma\text{-Al}_2\text{O}_3$, $\alpha\text{-Al}_2\text{O}_3$), boehmite ($\gamma\text{-AlOOH}$) and diasporite ($\alpha\text{-AlOOH}$). The gamma alumina

surface is analogous to the edge faces on gibbsite and its adsorption behavior is believed to be similar (Goldberg et al., 1996).

Variability of gibbsite in terms of grain size and surface area makes inter-experimental comparisons difficult. Measurements of percentage of specific surface area represented by edge faces (Hingston et al., 1972; Russell et al., 1974; Kavanagh et al., 1975; Parfitt et al., 1977; Sposito, 1984; van Riemsdijk and Lijklema, 1980; Goldberg et al., 1996) have revealed these differences. The variability can be traced to the analytical method of measurement and the history of the gibbsite (i.e., synthesis, pretreatment, grinding; Davis and Kent, 1990).

The solubility of gibbsite is pH dependent with a minimum at pH ~ 6 (Roberson and Hem, 1969; May et al., 1979). In artificial seawater, complexation by sulfate and fluoride anions increases gibbsite solubility (Sanjuan and Michard, 1987). Complexation with these anions decreases as pH increases so that solubility differences between distilled water and artificial seawater are negligible above pH 6.5 (Figure 1.2).

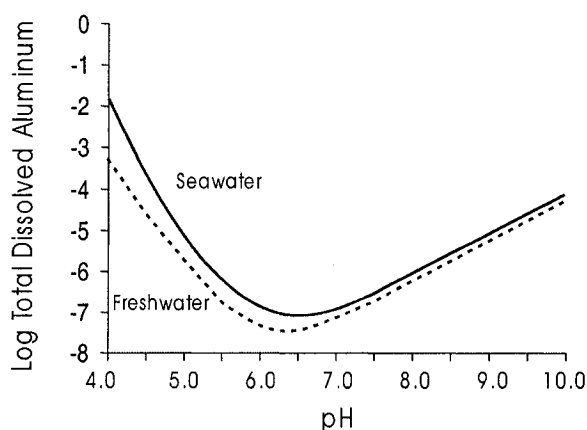


Figure 1.2 Calculated solubility of gibbsite in freshwater and seawater (S = 35) using the compilation of Stumm & Morgan (1996).

Thermodynamic calculations indicate that, in the presence of elevated [Si] concentrations such as recorded in the Fjord sediment porewaters ($\sim 150 \mu\text{M}$; Mucci and Edenborn, 1992), gibbsite should convert to kaolinite or albite (Figure 1.3) but field observations (S. Alpay, pers. comm.) as well as laboratory experiments (Crane, 1998) clearly indicate that it gibbsite is metastable and reacts very slowly (Su and Harsh, 1994).

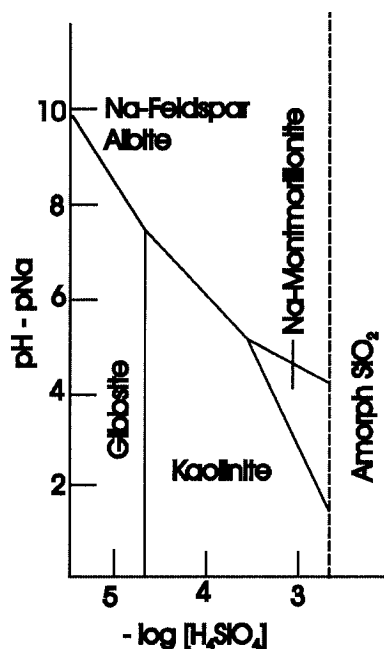


Figure 1.3 Activity-activity (predominance) diagram illustrating the field of stability of gibbsite (Stumm and Morgan, 1981).

1.4 Adsorption of Arsenate and Phosphate

Relatively consistent adsorption envelopes for both arsenic and phosphate have been reported for a number of aluminum substrates (Hingston et al., 1971; Chen et al., 1972; Huang, 1975; Anderson et al., 1976; Xu et al., 1991; Okazaki et al., 1989; Violante et al., 1991; Manning and Goldberg, 1996). Peak adsorption occurs at pH 6.5 and there is no narrow adsorption edge at pH 9-10 corresponding to the point of zero charge of

gibbsite (pH_{pzc} ; the pH at which the net surface charge is equal to zero). This behavior is typical of inner-sphere adsorption where changes in adsorption with pH are related to adsorbate speciation and to the charge of the solid surface.

Arsenate in sediments is commonly found in association with iron oxy-hydroxides (Maher, 1984; Belzile, 1988; Belzile and Tessier, 1990; De Vitre et al., 1991; Widerlund and Ingri, 1995), manganese oxides (Peterson and Carpenter, 1986) and aluminum compounds (Crecelius, 1975). **The established affinity of arsenate and phosphate for Al-oxides and the presence of aluminum rich particles in the Saguenay River and Fjord leads to the hypothesis that Al phases may serve as vectors of As and P and are responsible for their enrichment in the sediments of the Saguenay Fjord.**

A large number of adsorption studies of arsenate and phosphate onto a variety of solids have been undertaken but at concentrations that are two to three orders of magnitude larger than those encountered in most natural aquatic environments. Adsorption of phosphate to gibbsite (Bache, 1964; Muljadi et al., 1966; Helyar et al., 1976b; Parfitt et al., 1977), α -alumina (Chen et al., 1972; Halter and Pfeifer, 2001), γ -alumina (Huang, 1975) and non-crystalline aluminum oxide (Violante et al., 1991) in low ionic strength solutions have been described by Langmuir isotherms (Kinniburgh, 1986). Phosphate adsorption onto these solids has been described as a multi-staged process, usually fast adsorption followed by slower uptake (van Riemsdijk and Lijklema, 1980; Bache, 1964; Kuo and Lotse, 1974; Helyar et al., 1976b; Kyle et al., 1975).

Anderson et al. (1976) described arsenate adsorption on amorphous aluminum hydroxides in low ionic strength solutions by a Langmuir isotherm. Both linear and Langmuir isotherms can be calculated from published data on its adsorption onto amorphous aluminum hydroxides (Anderson and Malotky, 1979). Arsenate has been

reported to adsorb rapidly to these hydroxides as well as soils (Anderson et al., 1976; Xu et al., 1988; Livesey and Huang, 1981; Halter and Pfeifer, 2001).

1.5 Adsorption in the Presence of Seawater Constituents

A different chemical composition and a considerable increase in ionic strength suggest that the adsorption behavior of arsenate and phosphate on gibbsite in seawater should be markedly different than in freshwater. Surface complexation theory predicts that the presence of an indifferent electrolyte should decrease outer-sphere adsorption but should not affect the adsorption behavior of species that form inner-sphere surface complexes. For example, Okazaki et al. (1986) and Goldberg et al. (1993) reported that adsorption of Cu(II) and boron in the form of borate ($B(OH)_4^-$) on gibbsite was not affected by ionic strength for $0.1 < I < 1$. Although aluminum phases have been postulated as active “scavengers” for a variety of elements, adsorption studies in seawater are scarce.

Complexation and ion pairing of the adsorbate with seawater constituents may reduce adsorption. There is significant ion pairing between orthophosphate and both Mg and Ca in seawater (Turner et al., 1981; Millero and Schreiber, 1982). The same ion-pairs are predicted for arsenate (Lowenthal et al., 1977; Whiting (1992) in Langmuir et al., 1999). The nature of arsenate complexes in seawater has not been conclusively determined and there is some controversy about the existence of arsenate-fluoride complexes (Turner et al., 1981; Crecelius et al., 1986).

The limited number of adsorption sites on the gibbsite surface generates competition for the sites. It has been suggested that most electrolyte ions will form complexes with surface hydroxyls on oxides (Davis and Kent, 1990); the level of adsorption of any one ion will be a function of both its concentration and chemical

affinity. Ions that are not strictly electrostatically adsorbed, that is, display a specific affinity for the site or form inner-sphere complexes with some degree of covalent bonding will be adsorbed out of proportion to their concentration.

Hingston et al. (1972) showed that chloride ions adsorb non-specifically to gibbsite whereas adsorption of arsenate to an Al-rich soil was unaffected by the addition of chloride or sulfate (Hingston et al., 1972, Livesey and Huang, 1981). Sulfate at low pH (i.e., pH < 6) reduces arsenate adsorption on α -alumina (Xu et al., 1988). Helyar et al. (1976b) reported that bicarbonate at a lower concentration than seawater has no measurable effect on phosphate adsorption on gibbsite whereas Van Geen et al. (1994) reported that the presence of carbonate reduces Cr adsorption on goethite.

According to Huang and Stumm (1973), magnesium, calcium, and strontium are specifically adsorbed to α -alumina. The adsorption of univalent cations has not been investigated directly but their lack of effect on phosphate adsorption (Helyar et al., 1976b) suggests minimal and non-specific adsorption. The presence of calcium and magnesium (Chen et al., 1972; Helyar et al., 1976b) increases phosphate adsorption to aluminum oxides as was observed for goethite (Gao and Mucci, 2001, 2002). The addition of strontium nitrate to an aqueous solution has also been shown to increase phosphate adsorption (Helyar et al., 1976a). All three divalent cations are major constituents of seawater and Ca and Mg form strong ion pairs with phosphate (Millero and Schreiber, 1982) and possibly stable ternary surface complexes on metal oxides (Yao and Millero, 1996; Gao and Mucci 2001, 2002).

The interaction between fluoride and aluminum is strong (Elrashidi and Lindsay, 1986) and is responsible for an increase in gibbsite solubility in seawater (Sanjuan and

Michard, 1987). This interaction may also play a significant role in adsorption. A number of studies (Hingston et al., 1971; Hingston, 1981; Farrah et al., 1987) have shown strong adsorption of fluoride to gibbsite from dilute solutions. The removal of fluoride from aqueous solutions by activated alumina is widely used in wastewater treatment and is unaffected by salinity (Choi and Chen, 1979; Hao and Huang, 1986). Fluoride is also reported to cause phosphate desorption from gibbsite (Kuo and Lotse, 1974).

1.6 Objectives

The aim of this study is to measure the adsorption capacity of gibbsite for arsenate and phosphate in solutions of different composition and ionic strengths and predict the fate of both elements during estuarine mixing. Preliminary work (Fitzpatrick, 1998) suggested that the fluoride ion (F^-), a major, conservative constituent of seawater (> 1 ppm), may inhibit arsenate and phosphate adsorption onto gibbsite from seawater. Fluoride ions may either compete with other anions for the OH_2^+ surface sites (pH_{PZC} for gibbsite @ $pH = 9.8$) or substitute for the hydroxyl on the surface of gibbsite (Bower and Hatcher, 1967). Jambor et al. (1990) presented evidence for the formation of an Al-OH-F solid solution within the gibbsite structure and proposed its chemical formula to be $Al(OH,F)_3$. Based on these observations, we measured the adsorption capacity of gibbsite for arsenate and phosphate in pure water; 0.67 M NaCl; 10 mM $CaCl_2$; 10 mM $CaCl_2 + 0.64$ M NaCl and in artificial seawater ($S=35$) in the absence and presence of the fluoride ion. In the latter case, the fluoride activity of the experimental solutions was buffered by the addition of a fluorite (CaF_2) crystal to the reaction system.

We searched the literature to find the stoichiometric solubility (K_{sp}^*) of fluorite in seawater and, hence, derive the equilibrium fluoride concentration in this solution and

discovered that it has never been measured. Alternatively, it could be derived from the thermodynamic solubility constant (K_{sp}^0) of fluorite and the activity coefficients of the calcium and fluoride ions in seawater according to Equations 1.2 and 1.3 and assuming a pure solid phase fluorite:

$$K_{sp}^0 = (Ca^{2+})(F^-)^2 = [Ca^{2+}][F^-]^2 \gamma_{Ca^{2+}} \gamma_{F^-}^2 = K_{sp}^* \gamma_{Ca^{2+}} \gamma_{F^-}^2 \quad (1.2)$$

$$[F^-]_{eq} = \sqrt{\frac{K_{sp}^0}{[Ca^{2+}]_{sw} \gamma_{Ca^{2+}} \gamma_{F^-}^2}} \quad (1.3)$$

where K_{sp}^0 is the equilibrium thermodynamic solubility product; K_{sp}^* is the stoichiometric solubility product; () is the equilibrium activity of the ion; γ is the total ion activity coefficient; [] is the equilibrium total ion molal concentration and $[Ca^{2+}] = 10.65$ milli molal. Whereas the calcium activity coefficient in seawater (0.203) is well constrained by the $CaCO_3$ solubility measurements of Mucci (1983), the only estimate of the fluoride ion activity coefficient in seawater (0.296; Millero and Pierrot, 1998) was derived from measurements of the apparent dissociation constant of hydrofluoric acid (HF) in a NaCl- Na_2SO_4 - $MgCl_2$ - $CaCl_2$ -HCl solution at the ionic strength of seawater, under conditions (i.e. acidic pH) that are far from natural conditions (Culberson et al., 1970).

Nonetheless, using estimates of γ_{F^-} (0.296, Millero and Pierrot, 1998) and $\gamma_{Ca^{2+}}$ (0.203, Mucci, 1983) with a $K_{sp}^0 = 3.12 * 10^{-11}$ for fluorite (Robie et al., 1978) we estimated the $[F^-]_{eq}$ at 390 μM or 7.44 ppm. This value is close enough to the concentration of fluoride ions (i.e., 1.3 ppm, at $S = 35$) in seawater and justifies our use of fluorite as a suitable buffer for the adsorption experiments. Nevertheless, a determination of the K_{sp}^* of fluorite in seawater will allow us to accurately determine the $[F^-]_{eq}$ at $[Ca^{2+}]_{sw}$, and provide a better estimate of γ_{F^-} in seawater.

Consequently, fluorite equilibration experiments were carried out in a variety of solutions at 25⁰C and 1 atmosphere total pressure to address the effect of ionic strength and potential co-precipitation of a foreign ion on fluorite solubility as well as derive an estimate of the fluoride ion activity coefficient in seawater. To determine the effect of ionic strength, equilibrations were carried out in pure water, 0.1, 0.4 and 0.7 molar NaCl solutions. To investigate the effect of some major seawater constituents and possible co-precipitation, experiments were run in 10 mM CaCl₂ + 0.64 M NaCl (Na-Cl-Ca solution), 10 mM CaCl₂ + 0.484 M NaCl + 52 mM MgCl₂ (Na-Cl-Ca-Mg solution) and artificial seawater. In these latter solutions, equilibrium was approached from both undersaturation (i.e., initial [F⁻] = 0) and supersaturation (i.e., initial [F⁻] = 15 times the seawater value \cong 1 mM) to test for reversibility and confirm equilibrium. Measurements were carried out at pH \leq 7.5, thus the solutions are undersaturated with respect to calcite.

We used the ion-pairing model of Millero and Schreiber (1982); the Pitzer model of Millero and Pierrot (1998) and the PHREEQC v.2 computer code (Parkhurst and Appelo, 1999) to determine the activity coefficient of Ca²⁺ in the experimental solutions. The values determined by the above models in seawater will be compared to those values derived from the calcite solubility measurements of Mucci (1983), and factored in with K_{sp}^0 and K_{sp}^* measured in this study to estimate the fluoride ion activity coefficient in seawater.

1.7 References

- Abdullah, M. I., Shiyu, Z. and Mosgren, K., 1995. Arsenic and selenium species in the oxic and anoxic waters of the Oslofjord, Norway. *Marine Pol. Bull.*, 31: 116-126.
- Anderson, L.C.D. and Bruland, K.W., 1991. Biogeochemistry of arsenic in natural waters: The importance of methylated species. *Environ. Sci. Technol.*, 25: 420-427.
- Anderson, M. A., Ferguson, J. F. and Gavis, J., 1976. Arsenate adsorption on amorphous aluminum hydroxide. *J. Colloid Interface Sci.*, 54: 391-399.
- Anderson, M. A. and Malotky, D. T., 1979. The adsorption of protolyzable anions on hydrous oxides at the isoelectric pH. *J. Colloid Interface Sci.*, 72: 413-427.
- Andreae, M. O., 1978. Distribution and speciation of arsenic in natural waters and some marine algae. *Deep Sea Res.*, 25: 391-402.
- Bache, B. W., 1964. Aluminum and iron phosphate studies relating to soils II Reactions between phosphate and hydrous oxides. *J. Soil Sci.*, 15: 110-116.
- Barbeau, C., Bougie, R. and Côté, J.-E., 1981. Temporal and spatial variations of mercury, lead, zinc, and copper in sediments of the Saguenay Fjord. *Can. J. Earth Sci.*, 18: 1065-1074.
- Belzile, N. and Lebel, J., 1986. Capture of arsenic by pyrite in near-shore marine sediment. *Chem. Geol.*, 54: 279-281.
- Belzile, N., 1988. The fate of arsenic in sediments of the Laurentian Trough. *Geochim. Cosmochim. Acta*, 52: 2293-2302.
- Belzile, N. and Tessier, A., 1990. Interactions between arsenic and iron oxyhydroxides in lacustrine sediments. *Geochim. Cosmochim. Acta*, 54: 103-109.
- Bower, C.A. and Hatcher, J.T., 1967. Adsorption of fluoride by soils and minerals. *Soil Sci.*, 103: 151-154.
- Boyle, R. W. and Jonasson, I. R., 1973. The geochemistry of arsenic and its use as an indicator element in geochemical prospecting. *J. Geochem. Exploration*, 2: 251-296.
- Chen, Y. R., Butler, J.N. and Stumm W., 1972. Adsorption of phosphate on alumina and kaolinite from dilute aqueous solutions. *J. Colloid Interface Sci.*, 43: 421-436.
- Choi, W. W. and Chen, K. Y., 1979. The removal of fluoride from waters by adsorption. *J. Am. Water Works Assoc.*, 71: 562-570.
- Cossa, D., 1990. Chemical contaminants in the St. Lawrence Estuary and Saguenay Fjord. In: M.I. El-Sabh and N. Silverberg (Editors), *Oceanography of a Large Scale*

Estuarine System, The St. Lawrence. Coastal and Estuarine Studies, Springer-Verlag, 39: 239-268.

Crane, G., 1998. The stability of gibbsite in seawater. B.Sc. Thesis, McGill University.

Creclius, E. A., 1975. The geochemical cycle of arsenic in Lake Washington and its relation to other elements. *Limnol. Oceanogr.*, 20: 441-450.

Creclius, E. A., Bloom, N. S., Cowan C. E. and Jenne E. A., 1986. Speciation of selenium and arsenic in natural waters and sediments, Vol. 2. Electrical Power Research Institute, Research Project 2020-2, California.

Culberson, C., Pytkowicz, R.M. and Hawley, J.E., 1970. Seawater alkalinity determination by the pH method. *J. Mar. Res.* 28: 15-21.

Davis, J. A. and Kent, D. B., 1990. Surface complexation modeling in aqueous geochemistry. In: M. F. Hochella and A. F. White (Editors), *Mineral-Water Interface Geochemistry*. Mineralogical Society of America., 23: 178-260.

De Vitre, R., Belzile N. and Tessier A., 1991. Speciation and adsorption of arsenic on diagenetic iron oxyhydroxides. *Limnol. Oceanogr.*, 36: 1480-1485.

Drainville, G., 1968. La Fjord du Saguenay I Contribution à l'océanographie. *Naturaliste Canadien*, 95: 809-855.

Elrashidi, M.A. and Lindsay, W.L., 1986. Chemical equilibria of fluorine in soils: A theoretical development. *Soil Sci.*, 141: 275-280.

Farley, K.J. and Morel, F.M.M., 1986. Role of coagulation in sediment kinetics. *Environ. Sci. Technol.*, 20: 187-195.

Farrah, H., Slavek, J. and Pickering, W. F., 1987. Fluoride interactions with hydrous aluminum oxides and alumina. *Austral. J. Soil Res.*, 25: 55-69.

Fitzpatrick, A. J., 1998. The adsorption of arsenate and phosphate on gibbsite from artificial seawater. M.Sc. Thesis, McGill University.

Fortin, G. R. and Pelletier, M., 1995. Synthèse des connaissances sur les aspects physiques et chimiques de l'eau et des sédiments du Saguenay. Zone d'intervention prioritaire 22 et 23. Environnement Canada, région du Québec, Conservation de l'environnement, Centre St-Laurent. Rapport Technique.

Fowler, B.A., Ishiniski, N., Tsuchiya, K. and Vahter, M., 1979. Arsenic. In: L. Briberg (Editor), *Handbook on the Toxicology of Metals*. Elsevier-North-Holland Biomedical Press, pp. 293-319.

- Gagnon, C., Pelletier, E. and Maheu, S., 1993. Distribution of trace metals and some major constituents in sediments of the Saguenay Fjord., Canada. *Mar. Poll. Bull.*, 26: 107-110.
- Gagnon, C., Mucci, A., and Pelletier, E., 1995. Anomalous accumulations of acid volatile sulfides in a coastal marine sediment, Saguenay Fjord, Canada. *Geochim. Cosmochim. Acta*, 59: 2663-2677.
- Gagnon, C., Pelletier, E. and Mucci, A., 1997. Behaviour of anthropogenic mercury in coastal marine sediments. *Mar. Chem.*, 59: 159-176.
- Gao, Y. and Mucci, A., 2001. Acid base reactions, phosphate and arsenate complexation, and their competitive adsorption at the surface of goethite in 0.7 M NaCl solution. *Geochim. Cosmochim. Acta*, 65: 2361-2378.
- Gao, Y. and Mucci, A., 2002. Individual and competitive adsorption of phosphate and arsenate on goethite in artificial seawater. *Chem. Geol.* (In Press).
- Goldberg, S., Davis J. A., and Hem, J. D., 1996. The surface chemistry of aluminum oxides and hydroxides. In: G. Sposito (Editor), *The Environmental Chemistry of Aluminum*, CRC Press, Florida, pp. 271-331.
- Goldberg, S., Foster, H. S., and Heick E. L., 1993. Boron adsorption mechanisms on oxides, clay minerals, and soils inferred from ionic strength effects. *Soil Sci. Soc. Am. J.*, 57: 704-708.
- Gomez, E., Durillon, G.E., and Picot, B., 1999. Phosphate adsorption and release from sediments of brackish lagoons; pH, O₂ and loading influence. *Wat. Res.*, 10: 2437-2447.
- Gratton, S., 1995. Échanges entre le Saguenay et l'Estuaire du Saint-Laurent. *Profils Saguenay Vol.1,2*: 2-3.
- Halter, W.E. and Pfeifer, H.R., 2001. Arsenic (V) adsorption onto α -Al₂O₃ between 25 and 70°C. *Appl. Geochem.*, 16: 793-802.
- Hao, O. J. and Huang, C. P., 1986. Adsorption characteristics of fluoride onto hydrous alumina. *J. Environ. Engineer.*, 112: 1054-1069.
- Helyar, K. R., Munns, D. N. and Burau, R. G., 1976a. Adsorption of phosphate by gibbsite II Formation of a surface complex involving divalent cations. *J. Soil Sci.*, 27: 315-323.
- Helyar, K. R., Munns, D. N. and Burau, R. G., 1976b. Adsorption of phosphate by gibbsite. I. Effects of neutral chloride salts of calcium, magnesium, sodium, and potassium. *J. Soil Sci.*, 27: 307-314.

- Hingston, F. J., 1981. A review of anion adsorption. In: M. A. Anderson and A. J. Rubin (Editors) Adsorption of Inorganics at Solid-Liquid Interface. Ann Arbor Science, Ann Arbor, Michigan, pp. 51-90.
- Hingston, F. J., Posner, A. M. and Quirk, J. P., 1971. Competitive adsorption of negatively charged ligands on oxide surfaces. *Disc. Faraday Soc.*, 52: 334-342.
- Hingston, F. J., Posner, A. M. and Quirk, J. P., 1972. Anion adsorption by goethite and gibbsite. I. The role of the proton in determining adsorption envelopes. *J. Soil Sci.*, 23: 177-192.
- Huang, C. P., 1975. Adsorption of phosphate at the hydrous γ - Al_2O_3 -electrolyte interface. *J. Colloid Interface Sci.*, 53: 178-186.
- Huang, C. P. and Stumm, W., 1973. Specific adsorption of cations on hydrous α - Al_2O_3 . *J. Colloid Interface Sci.* 22: 231-259.
- Jambor, J.L., Sabina, A.P., Ramik, R.A. and Sturman, B.D., 1990. A fluorine-bearing gibbsite-like mineral from the Francon quarry, Montreal, Quebec. *Can. Min.*, 28: 147-159.
- Kavanagh, B. V., Posner, A. M. and Quirk, J. P., 1975. Effects of polymer adsorption on the properties of the electrical double layer. *Faraday Disc. Chem. Soc.*, 59: 242-249.
- Kinniburgh, D. G., 1986. General purpose adsorption isotherms. *Environ. Sci. Technol.*, 20: 895-904.
- Kraepiel, A.M.L., Chiffoleau, J.-F., Martin, J.-M. and Morel, F.M.M., 1997. Geochemistry of trace metals in the Gironde Estuary. *Geochim. Cosmochim. Acta*, 61: 1421-1436.
- Kuo, S. and Lotse, E. G., 1974. Kinetics of phosphate adsorption and desorption by hematite and gibbsite. *Soil Sci.*, 116: 400-406.
- Kyle, J. H., Posner, A. M. and Quirk, J. P., 1975. Kinetics of isotopic exchange of phosphate adsorbed on gibbsite. *J. Soil Sci.*, 26: 32-43.
- Langmuir, D., Mahoney, J., MacDonald, A. and Rowson, J., 1999. Predicting arsenic concentrations in the porewaters of buried uranium mill tailings. *Geochim. Cosmochim. Acta*, 63: 3379-3394.
- Lantzy, R. J. and Mackenzie, F. T., 1994. Tentative model of global oceanic cycling behaviour of arsenic. In: T. C. G. Hutchinson, C.A. and K. Meema (Editors), *Global Perspectives on Lead, Mercury and Cadmium Cycling in the Environment*. John Wiley Eastern Ltd. Publishers, New Delhi, India, pp. 95-114.

- Livesey, N. T. and Huang, P. M., 1981. Adsorption of arsenate by soils and its relation to selected chemical properties and anions. *Soil Sci.*, 131: 88-94.
- Loring, D.H. and Bowers, J.M., 1978. Geochemical mass balances for mercury in a Canadian fjord. *Chem. Geol.*, 22: 309-330.
- Loring, D.H., Rantala, R.T.T. and Smith, J.N., 1983. Response time of Saguenay Fjord sediments to metal contamination. *Environ. Biogeochem. Ecol. Bull.*, 35: 59-72.
- Lowenthal, D. H., Pilson, M. E. Q. and Byrne, R. H., 1977. The determination of the apparent dissociation constants of arsenic acid in seawater. *J. Marine Res.*, 35: 653-669.
- Lucotte, M. and d'Anglejan, B., 1988. Processes controlling phosphate adsorption by iron hydroxides in estuaries. *Chem. Geol.*, 67: 75-83.
- Maher, W. A., 1984. Mode of occurrence and speciation of arsenic in some pelagic and estuarine sediments. *Chem. Geol.*, 47: 333-345.
- Manning, B. A. and Goldberg, S., 1996. Modeling competitive adsorption of arsenate with phosphate and molybdate on oxide minerals. *Soil Sci. Soc. Am. J.*, 60: 121-131.
- May, H.M., Helmke, P.A. and Jackson, M.L., 1979. Gibbsite solubility and thermodynamic properties of hydroxy-aluminum ions in aqueous solution at 25°C. *Geochim. Cosmochim. Acta*, 43: 861-868.
- Millero, F.J. and Schreiber, D.R., 1982. Use of the ion pairing model to estimate activity coefficients of the ionic components of natural waters. *Amer. J. Sci.*, 282: 1508-1540.
- Millero, F.J. and Pierrot, D., 1998. A chemical equilibrium model for natural waters. *Aquatic Geochemistry* 4: 153-199.
- Morse, J. W., 1994. Interactions of trace metals with authigenic sulfide minerals: implications for their bioavailability. *Marine Chem.*, 46: 1-6.
- Mucci, A., 1983. The solubility of calcite and aragonite in seawater at various salinities, temperatures, and one atmosphere total pressure. *Amer. J. Sci.*, 283: 780-799.
- Mucci, A. and Edenborn, H. M., 1992. Influence of an organic-poor landside deposit on the early diagenesis of iron and manganese in a coastal marine sediment. *Geochim. Cosmochim. Acta*, 56: 3909-3921.
- Mucci, A., Richard, L.-F., Lucotte, M. and Guignard, C., 2000. The differential geochemical behaviour of arsenic and phosphorus in the water column and sediments of the Saguenay Fjord Estuary, Canada. *Aquat. Geochem.*, 6: 293-324.

- Muljadi, D., Posner, A. M. and Quirk, J. P., 1966. The mechanism of phosphate adsorption by kaolinite, gibbsite and pseudoboehmite. I. The isotherms and the effect of pH on adsorption. *J. Soil Sci.*, 17: 212-229.
- NRCC, 1978. Effects of arsenic in the Canadian environment. National Research Council of Canada Associate Committee On Scientific Criteria For Environmental Quality.
- Okazaki, M., Takamidoh, K., and Yamane, I., 1986. Adsorption of heavy metal cations on hydrated oxides and oxides of iron and aluminum with different crystallinities. *Soil Sci. Plant Nutrit.*, 32: 523-533.
- Okazaki, M., Sakaidani, K., Saigusa, T. and Sakaida, N., 1989. Ligand exchange of oxyanions on synthetic hydrated oxides of iron and aluminum. *Soil Sci. Plant Nutrit.*, 35: 337-346.
- Ouellet, M., 1979. Géochimie et granulométrie des sédiments superficiels du lac Saint-Jean et de la rivière Saguenay. INRS-Eau for Ministère de l'Environnement du Québec. Rapport no. 104.
- Parfitt, R. L., Fraser, A. R., Russell, J. D. and Farmer, V. C., 1977. Adsorption of hydrous oxides. II. Oxalate, benzoate, and phosphate on gibbsite. *J. Soil Sci.*, 26: 40-47.
- Parkhurst, D.L., Appelo, C.A.J., 1999. User's guide to PHREEQC (version 2). A computer program for speciation, batch-reaction, one-dimensional transport, and inverse geochemical calculations. U.S. Geological Survey Water-Resources Investigations Report 99-4259.
- Pelletier, E. and Canuel, G., 1988. Trace metals in surface sediment of the Saguenay Fjord, Canada. *Mar. Poll. Bull.*, 19: 336-338.
- Peterson, M. L. and Carpenter, R., 1986. Arsenic distributions in porewaters and sediments of Puget Sound, Lake Washington, the Washington coast and Saanich Inlet, B.C. *Geochim. Cosmochim. Acta*, 50: 353-369.
- Planas, D. and Healy, F. P., 1978. Effects of arsenate on growth and phosphorus metabolism of phytoplankton. *J. Phycol.*, 14: 337-341.
- Primeau, S., and Goulet, M., 1983. Résultats d'échantillonnage de l'eau et des sédiments de la baie des Ha! Ha! Ministère de l'Environnement du Québec. Direction générale des inventaires et de la recherche, service de la qualité des eaux.
- Richard, L. F., 1997. Comparaison des comportements géochimiques du phosphore et de l'arsenic dans le Fjord du Saguenay et l'Estuaire du St. Laurent. M.Sc. Thesis, Université du Québec à Montréal.

- Riedel, G. F., 1993. The annual cycle of arsenic in a temperate estuary. *Estuaries*, 16: 533-540.
- Roberson, C. E. and Hem, J. D., 1969. Solubility of aluminum in the presence of hydroxide, fluoride and sulfate. USGS Paper 1827-C.
- Robie, R.A., Hemingway, B.S., Fisher, J.R., 1978. Thermodynamic properties of Minerals and related substances at 298.15 K and 1 bar pressure and at higher temperatures. Geol. Surv. Bull., 1452, U.S. Government printing office, Washington D.C.
- Russell, J. D., Parfitt, R. L., Fraser, A. R. and Farmer, V. C., 1974. Surface structures of gibbsite, goethite and phosphated goethite. *Nature*, 248: 220-221.
- Sadiq, M., 1990. Arsenic chemistry in marine environments: a comparison between theoretical and field observations. *Mar. Chem.*, 31: 285-297.
- Sadiq, M., 1992. Toxic metal chemistry in marine environments. Marcel Dekker, New York.
- Sanders, J.G., 1983. Role of marine phytoplankton in determining the chemical speciation and biogeochemical cycling of arsenic. *Can. J. Fish. Aquat. Sci.*, 40: 192-196.
- Sanders, J.G. and Windom, H.L., 1980. The uptake and reduction of arsenic species by marine algae. *Estuar. Coast. Mar. Sci.*, 10: 555-567.
- Sanjuan, B. and Michard, G., 1987. Aluminum hydroxide solubility in aqueous solutions containing fluoride ions at 50°C. *Geochim. Cosmochim. Acta*, 51: 1823-1831.
- Saulnier, I. and Mucci, A., 2000. Trace metal remobilization following the resuspension of estuarine sediments: Saguenay Fjord, Canada. *Appl. Geochem.*, 15:191-210.
- Seibert, G. H., Trites, R. W., and Ried, S. J. , 1979. Deepwater exchange processes in the Saguenay Fjord. *J. Fish. Res. Board Can.*, 36: 42-53.
- Seyler, P. and Martin, J.M., 1990. Distribution of arsenite and total dissolved arsenic in major French estuaries: dependence on biogeochemical processes and anthropogenic inputs. *Mar. Chem.*, 29: 277-294.
- Sholkovitz, E.R., 1976. Flocculation of dissolved organic and inorganic matter during the mixing of river water and seawater. *Geochim. Cosmochim. Acta*, 40: 831-845.
- Sholkovitz, E.R., 1978. The flocculation of dissolved Fe, Mn, Al, Cu, Ni, Co, and Cd during estuarine mixing. *Earth Planet. Sci. Lett.*, 41: 77-86.
- Smedley, P.L. and Kinniburgh, D.G., 2002. A review of the source, behaviour and distribution of arsenic in natural waters. *Appl. Geochem.*, 17:517-568.

- Sposito, G., 1984. The surface chemistry of soils. Oxford University Press, New York.
- Stryer, L., 1988. Biochemistry. W.H. Freeman, New York.
- Stumm, W. and Morgan, J.J., 1981. Aquatic Chemistry: An Introduction Emphasizing Chemical Equilibria in Natural Waters. Wiley-Interscience, New York.
- Stumm, W. and Morgan, J.J., 1996. Aquatic Chemistry: Chemical Equilibria and Rates in Natural Waters. Wiley-Interscience, New York.
- Su, C. and Harsh, J. B., 1994. Gibbs free energies of formation at 298K for imogolite and gibbsite from solubility measurements. *Geochim. Cosmochim. Acta*, 58: 1667-1677.
- Sullivan, K.A. and Aller, R.C., 1996. Diagenetic cycling of arsenic in Amazon shelf sediments. *Geochim. Cosmochim. Acta*, 60: 1465-1477.
- Sundby, B. and Loring, D. H., 1978. Geochemistry of suspended particulate matter in the Saguenay Fjord. *Can. J. Earth Sci.*, 15: 1002-1011.
- Sundby, B., Gobeil, C., Silverberg, N. and Mucci, A., 1992. The phosphorous cycle in coastal marine sediments. *Limnol. Oceanogr.*, 37: 1129-1145.
- Therriault, J. C. and Lacroix, G., 1975. Penetration of the deep layer of the Saguenay Fjord by surface waters of the St. Lawrence Estuary. *J. Fish. Res. B. Can.*, 32: 2373-2377.
- Tremblay, G. H. and Gobeil, C., 1990. Dissolved arsenic in the St. Lawrence estuary and the Saguenay Fjord, Canada. *Marine Poll. Bull.*, 21: 465-468.
- Turner, D. R., Whitfield, M. and Dickson, A. G., 1981. The equilibrium speciation of dissolved components in freshwater and seawater at 25°C and 1 atmosphere pressure. *Geochim. Cosmochim. Acta*, 45: 855-881.
- Van Geen, A., Robertson, A.P. and Leckie, J.O., 1994. Complexation of carbonate species at the goethite surface; Implication for adsorption of metal ions in natural waters. *Geochim. Cosmochim. Acta*, 58: 2073-2086.
- van Riemsdijk, W. H. and Lijklema, J., 1980. Reaction of phosphate with gibbsite [Al(OH)₃] beyond the adsorption maximum. *J. Colloid Interface Sci.*, 76: 55-66.
- Violante, A., Colombo, C., and Buondonno, A., 1991. Competitive adsorption of phosphate and oxalate by aluminum oxides. *Soil Sci. Soc. Am. J.*, 55: 65-70.
- Waslenchuk, D.G., 1978. The budget and geochemistry of arsenic in a continental shelf environment. *Mar. Chem.*, 7: 39-52.

Widerlund, A. and Ingri, J., 1995. Early diagenesis of arsenic in sediments of the Kalix River estuary, northern Sweden. *Chem. Geol.*, 125: 185-196.

Whiting, K.S., 1992. The thermodynamics and geochemistry of arsenic, with application to subsurface waters at the Sharon Steel Superfund Site at Midvale, Utah. M.Sc. Thesis, Colorado School of Mines.

Xu, H., Allard B. and Grimvall, A., 1988. Influence of pH and organic substance on the adsorption of As(V) on geological materials. *Water Air Soil Poll.*, 40: 293-305.

Xu, H., Allard B. and Grimvall A., 1991. Effects of acidification and natural organic materials on the mobility of arsenic in the environment. *Water Air Soil Poll.*, 57-58: 269-278.

Yao, W. and Millero, F.J., 1996. Adsorption of phosphate on manganese dioxide in seawater. *Environ. Sci. Technol.*, 35: 536-541.

CHAPTER 2

The Influence of Ionic Strength and Fluoride Ion Concentration on the Adsorption Properties of Gibbsite: Phosphate and Arsenate Adsorption

Forward

Chapter 1 consisted of a general introduction encompassing the scope of the thesis as a whole and included background information critical to this work, which may not be directly referenced in the following manuscripts. Chapter 2 focuses on the experiments conducted to measure the adsorption capacity of gibbsite for arsenate and phosphate in solutions of different composition and ionic strengths in order to predict the fate of both elements during estuarine mixing. Particular attention was paid to the fluoride ion because of its status as a major seawater constituent and its known affinity for the gibbsite surface.

The Influence of Ionic Strength and Fluoride Ion Concentration on the
Adsorption Properties of Gibbsite: Phosphate and Arsenate Adsorption

Alain Garand and Alfonso Mucci

Department of Earth and Planetary Sciences
McGill University
3450 University Street
Montreal, Qc H3A 2A7
Canada
Fax: (514) 398-4680
Email: alm@eps.mcgill.ca

To be Submitted to Chemical Geology

2.1 Abstract

In estuarine environments, adsorption to suspended particulate matter is commonly cited as an important vector of trace elements to sediments. Gibbsite is a common component of riverine and estuarine suspended particulate matter and is recognized as a strong adsorbent of group V elements such as arsenic and phosphorus. In order to simulate the behavior of the adsorbent:adsorbate pair during estuarine mixing, the adsorption of arsenate and phosphate onto gibbsite from various solutions was measured as a function of the ionic strength and in the presence of major seawater constituents. Particular attention was paid to the fluoride ion because of its status as a major seawater constituent and its known affinity for the gibbsite surface.

In the absence of the fluoride ion, adsorption of both arsenate and phosphate is greatest in pure water and least in 0.67 M NaCl. Increasing ionic strength decreases adsorption of both anions while the presence of Ca in solution partially counteracts the decrease. The increase in adsorption in the presence of Ca is attributed to the formation of ternary complexes between Ca, phosphate or arsenate, and the gibbsite surface. In the presence of the fluoride ion, arsenate adsorption increases in all experimental solutions relative to pure water whereas the adsorption of phosphate decreases when compared to pure water. This differential adsorption behavior is attributed to the formation of arsenate-fluoride aqueous complexes with high affinity for the gibbsite surface. Adsorption data for both adsorbates were fit to the Freundlich isotherm equation. Freundlich distribution coefficients (K_F) generally corroborated the relative adsorption densities in each experimental solution.

Results of this study indicate that, with respect to their affinity for the gibbsite surface, the adsorption behavior of arsenate and phosphate is de-coupled during estuarine mixing.

2.2 Introduction

Gibbsite [α -Al(OH)₃] is the most common of the hydrated aluminum oxide minerals. It is usually the major component of bauxite and is a common soil constituent. It is recognized as a strong adsorbent of group V elements such as arsenic and phosphorous from solutions of low ionic strength (i.e., river waters and groundwaters) (Hingston et al., 1971; Chen et al., 1972; Huang, 1975; Anderson et al., 1976; Okazaki et al., 1989; Violante et al., 1991; Xu et al., 1991; Manning and Goldberg, 1996) but the fate of these and other adsorbates during estuarine mixing, where the ionic strength and the compositional complexity of the aqueous solution increases, has received little attention. Gibbsite is a common component of riverine and estuarine suspended particulate matter and, consequently, the behavior of adsorbed arsenate and phosphate on the gibbsite surface during estuarine mixing warrants more study.

The “edge” planes as opposed to the basal planes of gibbsite are believed to contain the only adsorption sites on the mineral surface (Parfitt et al., 1977; Russell et al., 1974). The hydroxyls on the edge planes coordinate to a single Al³⁺ ion and the excess charge retains water molecules. An adsorbed hydroxyl group replaces the bound water molecule (Goldberg et al., 1996) resulting in an aluminol surface complex (Al≡OH). The protonation and deprotonation of the complex can be described by reactions 2.0 and 2.1 (Manning and Goldberg, 1996) where pK^s represent the intrinsic equilibrium surface constants generated by the constant capacitance model (Stumm and Morgan, 1996).



The solubility of gibbsite is pH dependent with a minimum at pH 6 (Roberson and Hem, 1969; May et al., 1979). In artificial seawater, complexation by sulfate and fluoride anions increases gibbsite solubility (Sanjuan and Michard, 1987). Complexation with these anions decreases as pH increases so that solubility differences between distilled water and artificial seawater are negligible above pH 6.5.

Arsenic and phosphorus are both group V elements and, thus, have similar chemical properties and display similar geochemical behaviors. Both are released into aquatic and terrestrial environments from natural and anthropogenic sources and can be removed from solution by biotic uptake, adsorption, and precipitation. Thermodynamic calculations (Sadiq, 1992; Riedel, 1993; Abdullah et al., 1995) and field observations confirm that the inorganic arsenate ion, As(V), is the dominant species in oxygenated waters although lesser concentrations of arsenite, As(III) and methylated arsenicals have also been reported (Andreae, 1978; Waslenchuk, 1978; Sanders and Windham, 1980; Sanders, 1983; Seyler and Martin, 1990; Anderson and Bruland, 1991). Arsenate is often taken in lieu of phosphate by aquatic organisms, particularly in phosphate deprived environments, leading to an inhibition of oxidative phosphorylation and growth (NRCC, 1978; Planas and Healy, 1978; Stryer, 1988). Toxicity is highest for the reduced (As(III)) species of arsenic and less so for As (V) and organic arsenicals (Fowler et al., 1979) and manifests itself in humans who have been exposed to arsenic contaminated drinking

water through lung and skin cancer, hyperpigmentation, keratosis and vascular disorders (Fowler et al., 1979).

The arsenic cycle is complex (Lantzy and Mackenzie, 1994) and its ultimate sink is ocean sediment through adsorption to and slow absorption within authigenic iron and manganese oxyhydroxides that accumulate at or above the oxic-suboxic boundary (Sullivan and Aller, 1996). Precipitation in most sedimentary environments is insignificant except under anoxic conditions where reduced sulfur limits arsenic solubility (Widerlund and Ingri, 1995; Smedley and Kinniburgh, 2002). In most sedimentary environments, where reactive Fe is abundant, arsenic will co-precipitate with acid volatile sulfides (AVS) and pyrite (Boyle and Jonasson, 1973; Belzile and Lebel, 1986; Saulnier and Mucci, 2000).

Phosphorus is an essential nutrient to photosynthetic plants. At high concentrations, it is often considered a contaminant since it promotes excessive plant growth in freshwater. The decay of the plant material and the concomitant depletion of dissolved oxygen leads to eutrophication (Gomez et al., 1999). The only stable redox state of phosphorus in aqueous solutions is +V, thus inorganic phosphorus is always present as orthophosphate. The ultimate fate of phosphorus is ocean sediment through adsorption to and slow absorption within authigenic iron oxy-hydroxides that accumulate at or above the oxic-suboxic boundary and the precipitation of apatite (Sundby et al., 1992), but the major nutrient status of phosphorus is indicative of the complexity of the phosphorus cycle (Sundby et al., 1992).

A large number of studies on adsorption of arsenate and phosphate onto a variety of aluminum substrates have been undertaken but at concentrations that are two to three orders of magnitude larger than those encountered in most natural aquatic environments.

Adsorption of phosphate to gibbsite (Bache, 1964; Muljadi et al., 1966; Helyar et al., 1976b; Parfitt et al., 1977), α -alumina (Chen et al., 1972, Halter and Pfeifer, 2001), γ -alumina (Huang, 1975) and non-crystalline aluminum oxide (Violante et al., 1991) in low ionic strength solutions have been described by Langmuir isotherms (Kinniburgh, 1986). Phosphate adsorption onto these solids has been described as a multi-staged process, usually fast adsorption followed by slower uptake (van Riemsdijk and Lijklema, 1980; Bache, 1964; Kuo and Lotse, 1974; Helyar et al., 1976b; Kyle et al., 1975).

Anderson et al. (1976) described arsenate adsorption on amorphous aluminum hydroxides in low ionic strength solutions by a Langmuir isotherm. Both linear and Langmuir isotherms can be calculated from published data on its adsorption on amorphous aluminum hydroxides (Anderson and Malotky, 1979). Arsenate has been reported to adsorb rapidly to these hydroxides as well as soils (Anderson et al., 1976; Xu et al., 1988; Livesey and Huang, 1981; Halter and Pfeifer, 2001).

Although aluminum phases (i.e., oxides and clays) have been postulated as active “scavengers” for a variety of elements, adsorption studies in the presence of major seawater constituents and in seawater are scarce. Hingston et al. (1972) showed that chloride ions adsorb non-specifically to gibbsite whereas Huang and Stumm (1973) reported that magnesium, calcium, and strontium are specifically adsorbed to α -alumina. Adsorption of arsenate to an Al-rich soil was unaffected by the addition of chloride or sulfate (Hingston et al., 1972, Livesey and Huang, 1981), whereas Xu et al., (1988) reported that sulfate at low pH (pH < 6.0) reduces arsenate adsorption on α -alumina. The presence of calcium and magnesium (Chen et al., 1972; Helyar et al., 1976b) increases phosphate adsorption to aluminum oxides as was observed for goethite (Gao and Mucci,

2001, 2002) and the addition of strontium nitrate to an aqueous solution has also been shown to increase phosphate adsorption (Helyar et al., 1976a). All three divalent cations are major constituents of seawater and Ca and Mg form strong ion pairs with phosphate (Millero and Schreiber, 1982) and possibly stable ternary surface complexes on metal oxides (Yao and Millero, 1996; Gao and Mucci 2001, 2002).

The interaction between fluoride and aluminum is strong (Elrashidi and Lindsay, 1986) and is responsible for an increase in gibbsite solubility in seawater (Sanjuan and Michard, 1987). A number of studies (Hingston et al., 1971, Hingston, 1981; Farrah et al., 1987) have shown strong adsorption of fluoride to gibbsite from dilute solutions. The removal of fluoride from aqueous solutions by activated alumina is widely used in wastewater treatment and is unaffected by salinity (Choi and Chen, 1979; Hao and Huang, 1986). Fluoride is also reported to cause phosphate desorption from gibbsite (Kuo and Lotse, 1974).

Preliminary work (Fitzpatrick, 1998) suggested that the fluoride ion (F^-), a major, conservative constituent of seawater (> 1 ppm), might inhibit arsenate and phosphate adsorption onto gibbsite from seawater. Fluoride ions may either compete with other anions for the OH_2^+ surface sites (pH_{PZC} for gibbsite @ $pH = 9.5$) or substitute for the hydroxyl on the surface of gibbsite (Bower and Hatcher, 1967). Jambor et al. (1990) presented evidence for the formation of an Al-OH-F solid solution within the gibbsite structure and concluded its chemical formula to be $Al(OH,F)_3$. On the basis of these previous investigations, we measured the adsorption of arsenate and phosphate on gibbsite in a variety of experimental solutions including artificial seawater, in order to

characterize the influence of ionic strength, solution composition and, more specifically, the presence of fluoride ions on their adsorption behaviors.

2.3 Materials and Methods

Chemical reagents used for all experiments and analytical procedures were reagent grade or better. Specific grades were used as required by some techniques and are described thoroughly in the relevant sections. All glassware and reusable plasticware were rinsed with Nanopure™ water after soaking in a 10% HNO₃ (glassware) or 10% HCl (Plasticware) acid bath for at least 12 hours. Millipore Nanopure™ water was used for preparation of all solutions except where indicated.

A bulk sample of gibbsite powdered to less than 500 microns was obtained from Alcan Inc. The gibbsite was cleaned by soaking in 1 N HCl for 24 hours followed by multiple rinses with Nanopure™ water. It was then oven-dried at 110° C for a period of 24 hours. Powder x-ray diffraction analysis performed with a RIGAKU D/Max 2400 X-ray diffractometer showed a perfect match to reference gibbsite (JCPDS 29-0041). X-ray fluorescence analysis of the powder, using a Philips PW2400 3kW automated XRF spectrometer system with a Rhodium 60 kV end window x-ray tube (Table 2.0) revealed only minor silica and sodium impurities. Phosphorus (as P₂O₅) content was 0.005 % and arsenic was below the detection limit (1 ppm) of the instrument.

Table 2.0 Gibbsite major and trace element composition (XRF)

SiO ₂	0.25%	CaO	0.03%	Cu	10 ppm
TiO ₂	0.01%	Na ₂ O	0.35%	Ni	3 ppm
Al ₂ O ₃	64.94%	K ₂ O	0.03%	Sb	2.8 ppm
Fe ₂ O ₃	0.08%	P ₂ O ₅	0.005%	Ge	2.7 ppm
MnO	0.03%	Cr ₂ O ₃	15 ppm	LOI	34.34%

The specific surface area of the gibbsite, 0.17 m²/g, was determined by multi-point BET N₂ adsorption with a Autosorb-6 Physisorption Analyzer (Quantachrome Corp. Boynton Beach, Florida).

Fluorite crystals used to buffer some of the experimental solutions with respect to the fluoride ion activity (see below) were obtained from Wards, Fluorite # 46 E 3113. X-ray fluorescence analysis (Table 2.1) indicated only minor silica and sodium impurities. Phosphorus (as P_2O_5) content was reported at 0.01% and arsenic was below the detection limit of 1 ppm.

Table 2.1 Fluorite major and trace element composition (XRF)

SiO ₂	1.11%	CaO	70.72%	Cr ₂ O ₃	33 ppm
TiO ₂	0.01%	Na ₂ O	0.09%	V	< d/l
Al ₂ O ₃	0.06%	K ₂ O	< d/l	Zn	< d/l
Fe ₂ O ₃	0.05%	P ₂ O ₅	0.01%	As	< d/l
MnO	< d/l	BaO	< d/l	LOI	28.03%

Artificial seawater was prepared in 5 or 10 kg batches according to the recipe of Kester et al. (1969) except that NaF was omitted and NaHCO₃ was added as required to adjust the pH. The seawater was prepared with distilled water. The stock solutions of volumetric salts (MgCl₂, CaCl₂ and SrCl₂) were standardized with a silver nitrate solution, itself standardized against a solution prepared gravimetrically from NaCl salt dried at 110 °C for at least 24 hours and stored in a vacuum dessicator. The salinities of all seawater solutions used were 35.0 ± 0.5 as determined by titration with a silver nitrate solution standardized against IASPO standard seawater.

Solutions of 10 mM CaCl₂, 0.67 M NaCl and mixed 10 mM CaCl₂ + 0.64 M NaCl were prepared according to the procedures described above. Arsenate and phosphate concentrations in the experimental solutions were below detection limits (see below). Ten millimolar arsenate and phosphate stock solutions were prepared by dissolution of As₂O₅·3H₂O and KH₂PO₄ salts in Nanopure™ water. The phosphate stock solution was prepared fresh as required whereas the arsenic stock solution was stored refrigerated for

periods of up to 3 months. Stock solutions were diluted with the experimental solutions; 0.67 M NaCl; 10 mM CaCl₂; 10 mM CaCl₂ + 0.64 M NaCl and in artificial seawater to an intermediate concentration of 100 μM. From the intermediate solution concentration, nominal concentrations were obtained. Adsorption experiments were also carried out in Nanopure™ water for comparison purposes.

Adsorption experiments were carried out in batch reactors, 50 ml glass (phosphate) or plastic (arsenate) centrifuge tubes at room temperature (23 ± 1°C). Fifty milligrams of pre-washed gibbsite were added to 40ml of each experimental solution at 0, 1, 2, 5, 10, 20 and 50 μM arsenate and phosphate concentrations. A twin series of samples was set up in which a fluorite crystal of ~ 0.25 cm³ was added to each reaction vessel in order to buffer the solutions with respect to the fluoride ion activity. Each set of experiments included a gibbsite-free sample typically at 20 μM AsO₄ and PO₄ to evaluate adsorption by container walls.

The pH of each solution was adjusted before the experiments and after 48 and 72 hours of equilibration to ~7.0 by addition of micro amounts of 0.1 M NaOH or 10% HCl. All pH measurements were carried out using a Radiometer Copenhagen PHM 84 pH meter with an Ag/AgCl combination pH electrode calibrated against three NIST-traceable buffers at pH 4.00, 7.00 and 10.00. The pH of a TRIS buffer solution prepared in artificial seawater or TRIS buffer in > 0.1 M NaCl solutions (Millero et al., 1987, 1993) were used in order to convert all measurements to the total hydrogen concentration scale. Glass tubes were sealed with double layers of Parafilm™ whereas plastic tubes were sealed with the accompanying screw caps. All tubes were shaken by hand once a day.

Preliminary adsorption experiments were run for 15 days with sampling after 1, 3, 5, 10 and 15 days of equilibration. As equilibrium was reached within 10 days, subsequent runs were sampled after 7 and 15 days. Fitzpatrick (1998) and Anderson et al. (1976) observed that under similar experimental conditions, equilibrium was reached within 7 days.

On sampling dates, pH was measured first and solutions were withdrawn from the tubes with a 60 ml plastic syringe. After rinsing the syringe with the experimental solution, an aliquot was filtered through a 0.45 μm MSI Acetate Plus or Millipore™ HA filter into either a 30 mL Nalge™ high-density polyethylene bottle (arsenate) or a 20 mL glass scintillation vial (phosphate). Samples for arsenate, aluminum and fluoride analyses were preserved by the addition of a 1% equivalent volume of concentrated, high purity HCl (Seastar™) and refrigerated. Insignificant losses of As(V) have been reported for 100 nM artificial seawater solutions stored in glass, high density polyethylene and PTFE containers for periods of up to 28 days (Masse et al., 1981). Phosphate analyses were carried out on the sampling day.

Total arsenic concentrations was determined by the hydride generation/atomic absorption spectrometric (AAS) method described by Aggett and Aspell (1976) using a Perkin Elmer 5100 AAS equipped with a FIAS 200 flow injection system and an AS 90 autosampler. Tests confirmed that there are insignificant matrix effects between the experimental solutions and aqueous standards thus samples were diluted volumetrically with Nanopure™ water to bring samples into the operational range of the method (2–20 ppb). Aqueous standard solutions were prepared the day prior to analysis from a certified NIST traceable standard of 1000 ppm (BDH A.A. standard). The correlation coefficient of the least squares fit, r^2 , to the calibration curve was always above 0.9990. The

detection limit for this procedure is 1.4 nmol/L and the relative standard deviation (RSD) of three replicate analyses was generally below 5%.

A Hewlett Packard 8453 UV-Visible spectrophotometer and 10 mm quartz cuvette were used for the phosphate, aluminum and fluoride analyses. Phosphate was determined by the heptamolybdate spectrophotometric method of Koroleff (1976). The detection limit and linear range of this method are reported as 0.01 $\mu\text{mol/L}$ and 0.01 to 28 $\mu\text{mol/L}$, respectively. Calibrations were conducted for each analytical session using dilute KH_2PO_4 stock solutions prepared on the day of the analyses and matrix-matched with those of the experimental solutions. The correlation coefficient, r^2 , of the calibration curve was always above 0.999. Standards were analyzed in triplicate and correction for blanks were made. Samples were measured in triplicate and RSD% values were under 5%.

A number of samples were analyzed for background aluminum concentrations within two months of sampling using the catechol violet spectrophotometric method of Dougan and Wilson (1974). The detection limits and linear range of this method are reported as 0.01 mg/L and 0.01 to 0.3 mg/L respectively. Calibration curves were established using aqueous standards prepared on the day of analysis from a 1000 ppm reference aluminum (Fisher Scientific reference # SA442-500) solution. Only the arsenate equilibrated samples were analyzed for dissolved aluminum since tests showed strong interference by phosphate. The correlation coefficient, r^2 , of the calibration curve was always above 0.995. Standards were analyzed in triplicate and correction for blanks were made. Samples were measured in triplicate and RSD% values were under 5%.

The Lanthanum (III)/Alizarin Fluorine Blue spectrophotometric method described by Hanocq and Molle (1968) was used to measure background F^- concentrations in the

fluoride buffered experiments. The detection limit and linear range of this method are reported as 0.075 mg/L and 0.075 mg/L to 1.2 mg/L, respectively. Calibrations were conducted for each analytical session using a gravimetrically prepared 100 ppm NaF stock solution. Standards were analyzed in triplicate and corrections for blanks were applied. R^2 values of the calibration curve were always above 0.995. Samples were measured in duplicate and RSD% values were generally under 5%. Calibration standards and samples were matrix-matched.

2.4 Results

Adsorption densities were calculated from the difference between the initial and equilibrated sample concentrations and the solid/solution ratio (S).

$$\Gamma = \frac{C_I - C_F}{S} \quad [2.2]$$

where	Γ	= adsorption density ($\mu\text{mol/g}$ of solid)
	C_I	= initial solution concentration of the adsorbate ($\mu\text{mol/l}$)
	C_F	= final solution concentration of the adsorbate ($\mu\text{mol/l}$)
	S	= solid:solution ratio (g/l)

The lack of intrinsic equilibrium constants that characterize the interaction of seawater constituents with the gibbsite surface limits us to the use of an empirical model. Although the results of such a model will not be directly applicable to other solutions, they will serve to unambiguously fulfill the objectives of this study and predict the fate of adsorbates associated with gibbsite during estuarine mixing. The empirical approach has been widely used in geochemical transport and other global models where the computational simplicity and low data requirements outweigh the greater applicability of an analytical approach (Bache, 1964; Anderson et al., 1976; Wu et al., 2002).

The empirical approach generates adsorption isotherms on the basis of an equation that provides a correlation or fitting coefficient between the amount of adsorbed solute and the equilibrium solute concentration. The isotherms generated in this study are fitted to the Freundlich and Langmuir equations.

A common form of the Freundlich isotherm equation is:

$$\Gamma_J = K_F [J]^\beta \quad [2.3]$$

where Γ_J is the adsorption density, K_F is the equilibrium Freundlich distribution coefficient or adsorption capacity, $[J]$ is the equilibrium adsorbate concentration and β is an empirical power coefficient which reflects the multiplicity of adsorption sites, thus, when $\beta = 1$ the isotherm is linear. A plot of $\text{Log } \Gamma_J$ vs. $\text{Log } [J]$ yields a straight line with the intercept equal to $\text{Log } K_F$ and the slope to β .

The Langmuir theory is based on a set of four assumptions: 1) the surface carries a finite number of adsorption sites; 2) all sites have identical energies or affinities for the adsorbate; 3) adsorption is limited to monolayer coverage; 4) the interaction with the surface is physical (i.e. electrostatic) rather than chemical (covalent). A common form of the Langmuir isotherm equation is:

$$\Gamma_J = \Gamma_{Max} \left[\frac{K_L [J]}{1 + K_L [J]} \right] \quad [2.4]$$

where Γ_{Max} is the maximum adsorption density and K_L is the equilibrium Langmuir coefficient. Γ_{Max} and K_L can be obtained from a plot of the reciprocal form of equation 2.4 as follows:

$$\Gamma_J^{-1} = \Gamma_{Max}^{-1} + K_L^{-1} \Gamma_{Max}^{-1} [J]^{-1} \quad [2.5]$$

Data fitting either theory does not necessarily mean that their underlying assumptions have been fulfilled. Rather, these equations are strictly empirical fits used to illustrate the data.

Isotherms were fitted to the data by least squares regression using Microsoft Excel™. The empirical parameters for the Freundlich isotherm equation were derived for each data subset by the goal seeking function of that program. Fits to the Langmuir

isotherm equation were checked by a linearization method (Vieth and Sposito, 1977). The coefficient of variation of the data based on randomly chosen duplicate samples ranged from 1.0 to 10%.

2.4.1 Arsenate Adsorption in the Absence of Fluoride

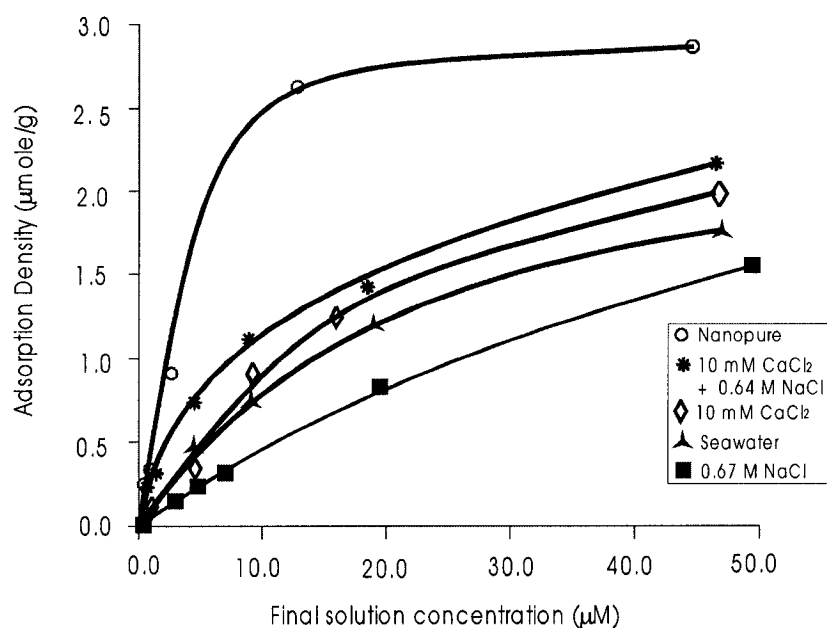


Figure 2.4.1 Adsorption isotherms of arsenate onto gibbsite in F free solutions after 15 days @ 23 ± 1 °C and $\text{pH } 7.2 \pm 0.10$.

Arsenate adsorption isotherms in the fluoride-free solutions are shown in Figure 2.4.1. The arsenate adsorption pattern in Nanopure™ water is consistent with results of other studies (Anderson et al., 1976; Anderson and Malotky, 1979). The maximum adsorption density of the gibbsite, $2.66 \mu\text{mol/g}$ (Table 2.4.1), is lower than values reported in other studies but in the absence of data on specific surface areas of the gibbsite used the comparison is meaningless. The specific surface area of the gibbsite used in this study is $0.17 \text{ m}^2/\text{g}$, thus, the maximum adsorption density translates into 1.56

* 10^{-5} $\mu\text{mole}/\text{m}^2$. If we factor in the average specific surface area of synthetic gibbsite reported in the literature (i.e., $120 \text{ m}^2/\text{g}$; Langmuir, 1997) to the arsenate adsorption density of $1180 \mu\text{mole}/\text{g}$ reported by Anderson et al. (1976) at pH 7.0, an adsorption density of $9.83 * 10^{-6} \mu\text{mole}/\text{m}^2$ is obtained, a value close to the one reported in this study.

Figure 2.4.1 shows that arsenate adsorption onto gibbsite in the other fluoride-free solutions is significantly diminished with respect to that measured in Nanopure™ water and the isotherms do not plateau over the range of As concentrations investigated in this study. Reduced adsorption in the 0.67 M NaCl solution, an indifferent electrolyte with respect to the gibbsite surface, may indicate that interactions of the adsorbate with the gibbsite surface is partially electrostatic or that the presence of Na^+ stabilizes arsenate in solution. The presence of other major seawater constituents, Ca in particular, appears to partially counteract the decrease in adsorption caused by the increase in ionic strength or the addition of NaCl.

The fluoride-free arsenate adsorption data were fitted to both the Freundlich and Langmuir isotherm equations and fitting parameters are summarized in Table 2.4.1. As shown in the table, linear regression coefficients (r^2) for the different solutions are larger than 0.838, indicating that both the Langmuir and Freundlich equations successfully describe the adsorption of arsenate on the gibbsite surface from each solution. The maximum arsenate adsorption on gibbsite in the absence of fluoride ions occurs in Nanopure™ water and fits a Langmuir isotherm (Fig. 2.4.1) with an excellent goodness of fit ($r^2 = 0.930$). The Langmuir coefficient (K_L) is $5.60 * 10^{-4}$ and the total site density, Γ_{Max} , is $2.66 \mu\text{mole}/\text{g}$.

Table 2.4.1 Freundlich and Langmuir parameters of arsenate adsorption isotherms in fluoride-free solutions. The pH reported herein represents the average of all samples for each solution type.

	pH	K_F	β	r^2	K_L	S_T	r^2
Nanopure™	7.24 ± 0.06	1.00 * 10 ⁻²	0.805	0.898	5.60 * 10 ⁴	2.66 * 10 ⁻⁶	0.930
10 mM CaCl₂ + 0.64M NaCl	7.27 ± 0.13	0.38 * 10 ⁻²	0.581	0.953	2.48 * 10 ⁵	1.36 * 10 ⁻⁶	0.838
10 mM CaCl₂	7.06 ± 0.08	8.07 * 10 ⁻⁴	0.745	0.967	7.07 * 10 ⁴	1.86 * 10 ⁻⁶	0.988
Seawater	7.22 ± 0.05	4.89 * 10 ⁻⁴	0.560	0.984	5.66 * 10 ⁴	2.31 * 10 ⁻⁶	0.998
0.67M NaCl	7.22 ± 0.07	3.05 * 10 ⁻⁴	0.537	0.989	2.40 * 10 ⁵	1.00 * 10 ⁻⁶	0.958

The order in which the adsorption of arsenate decreases among the experimental solutions: 10 mM CaCl₂ + 0.64 M NaCl > 10 mM CaCl₂ > seawater > 0.67 M NaCl is reflected by the decreasing K_F values even though β values are different in each solution.

To compare the K_F values (adsorption capacity) for each solution on an equal footing, the data were re-fit with an averaged $\beta = 0.6 \pm 0.15$ and K_F re-calculated for each adsorption density-final adsorbate concentration pair. Averaged K_F for each experimental solution are presented in Table 2.4.2. The relative order of adsorption capacities between the solutions is again reflected quantitatively by decreasing K_F values at equivalent β .

Table 2.4.2 Re-calculated K_F values for each type of experimental solution with an average β of 0.6

	K_F
Nanopure™ water	1.2 ± 0.4 * 10 ⁻³
10 mM CaCl₂ + 0.64M NaCl	1.0 ± 0.2 * 10 ⁻³
10 mM CaCl₂	7.4 ± 1.0 * 10 ⁻⁴
Seawater	7.2 ± 0.5 * 10 ⁻⁴
0.67M NaCl	6.5 ± 0.8 * 10 ⁻⁴

Similarly, K_L values for each experimental solution were re-calculated by fitting the data with an $S_T = 2.66 * 10^{-6}$ for each adsorption density-final adsorbate concentration pair but failed to produce any meaningful results.

2.4.2 Arsenate Adsorption in the Presence of Fluoride

In the presence of fluoride ions, arsenate adsorption onto gibbsite (Figure 2.4.2) increases significantly in all solutions compared to Nanopure™ water and the isotherms are linear over the range of arsenate concentrations investigated in this study.

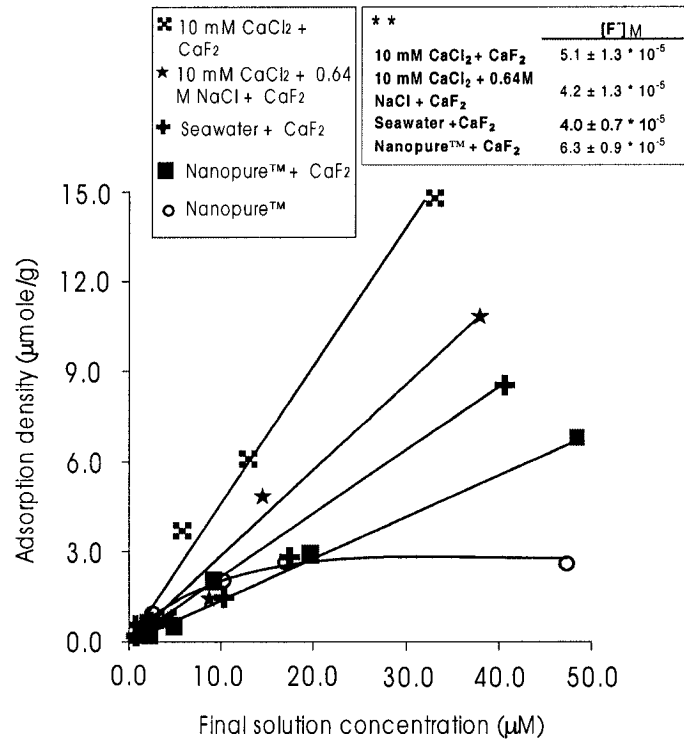


Figure 2.4.2 Adsorption isotherms of arsenate onto gibbsite in F⁻ buffered solutions after 15 days @ 23 ± 1 °C and pH 7.00 ± 0.15.
 **Averaged [F⁻] for all samples analyzed for each type of experimental solution.

Arsenate adsorption in the presence of F⁻ is greatest in 10 mM CaCl₂ followed by 10 mM CaCl₂ + 0.64 M NaCl, seawater and Nanopure™ water, respectively. Given that all the arsenate adsorption isotherms in F⁻-buffered solutions are linear, they can only be

fit to the Freundlich equation. Fitting parameters are summarized in Table 2.4.3 and all linear regression coefficients (r^2) for the different solutions are larger than 0.906.

Table 2.4.3 Freundlich parameters of arsenate adsorption isotherms in the fluoride-buffered solutions. The pH reported herein represents the average of all samples for each solution type.

	pH	K_F	β	r^2
10 mM CaCl₂ + F	7.00 ± 0.10	4.80 * 10 ²	1.63	0.937
10 mM CaCl₂ + 0.64M NaCl + F	6.93 ± 0.05	1.77 * 10 ¹	1.25	0.988
Seawater + F	7.08 ± 0.08	3.78 * 10 ⁰	1.30	0.978
Nanopure™ + F	6.97 ± 0.26	0.37 * 10 ⁰	1.07	0.906

The decreasing order of adsorption capacities in the presence of F⁻: 10 mM CaCl₂ > 10 mM CaCl₂ + 0.64 M NaCl > seawater > Nanopure™ water is reflected by the decreasing K_F values even though β values are different in each solution.

To compare the K_F values (adsorption capacity) for each solution on an equal footing, the data were re-fit with an averaged $\beta = 1.3 \pm 0.3$ and K_F re-calculated for each adsorption density-final adsorbate concentration pair. Averaged K_F for each experimental solution are presented in Table 2.4.4. The relative order of adsorption capacities between the different solutions is again reflected quantitatively with decreasing K_F values at equivalent β with the exception of Nanopure™ water and seawater which have reversed their order.

Table 2.4.4 Re-calculated K_F values for each type of experimental solution with an average β of 1.3

	K_F
10 mM CaCl₂ + F	10.5 ± 3.2
10 mM CaCl₂ + 0.64M NaCl + F	7.6 ± 1.3
Nanopure™ + F	5.5 ± 1.9
Seawater + F	3.7 ± 0.8

Fluoride concentrations were measured in each fluoride-buffered solution sample. Results were averaged for each solution type and are presented as an insert of Figure

2.4.2. These concentrations are very close to seawater values ($6.84 \times 10^{-5} \text{ M}$ @ $S = 35$) but are not at saturation (i.e., $3.3 \times 10^{-4} \text{ M}$) with respect to fluorite (see Chapter 3 of this thesis). Nonetheless, the $[\text{F}^-]$ measured are close enough to seawater values and, it is entirely reasonable to assume that a similar behavior would be observed in an open-seawater system (i.e. where F^- would not be depleted by adsorption to the gibbsite).

2.4.3 Phosphate Adsorption in the Absence of Fluoride

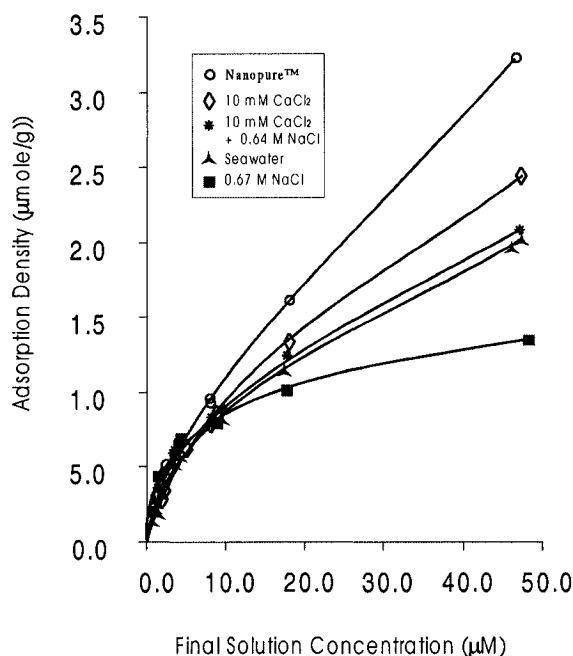


Figure 2.4.3 Adsorption isotherms of phosphate onto gibbsite in F^- free solutions after 15 days @ $23 \pm 1 \text{ }^\circ\text{C}$ and $\text{pH } 7.12 \pm 0.19$.

Figure 2.4.3 shows the phosphate adsorption isotherms in the fluoride-free solutions. Phosphate adsorption density is slightly greater than that of arsenate in the fluoride-free experimental solutions. The greater adsorption density of phosphate compared to arsenate on aluminum oxide substrates has been reported in other studies (Manning and Goldberg, 1996; Okazaki et al., 1989; Hingston et al., 1971). The greater affinity of phosphate for the gibbsite surface may be due to a size effect; a phosphate

surface complex (45 Å/anion) occupies less space than an arsenate surface complex (61 Å/anion) thus allowing greater adsorption density (Hingston, 1981), or may be indicative of a greater chemical affinity (covalency) between phosphate and the gibbsite surface.

In contrast to arsenate, phosphate adsorption on gibbsite does not plateau in the fluoride-free Nanopure™ water solution over the range of concentrations investigated in this study. Figure 2.4.3 shows that phosphate adsorption onto gibbsite in the other fluoride-free experimental solutions is significantly diminished with respect to Nanopure™ water. The greatest decrease in adsorption occurs in the 0.67 M NaCl solution, as was the case for arsenate adsorption. This decrease is attributed to the same mechanisms presented in Section 2.4.1 for arsenate adsorption. The presence of other major seawater constituents, Ca in particular, appears to partially counteract the decrease in adsorption caused by the increase in ionic strength as it did in the arsenate experiments.

Given the lack of an adsorption plateau in all the experimental solutions, the fluoride-free phosphate adsorption data were fitted with the Freundlich isotherm equation only, and fitting parameters are summarized in Table 2.4.5.

Table 2.4.5 Freundlich parameters of phosphate adsorption isotherms in fluoride-free solutions. The pH reported herein represents the average of all samples for each solution type.

	pH	K_F	β	r^2
Nanopure™	7.05 ± 0.14	3.26 * 10 ⁻⁴	0.493	0.900
10 mM CaCl₂	7.02 ± 0.19	3.08 * 10 ⁻⁴	0.420	0.910
Seawater	7.36 ± 0.08	2.97 * 10 ⁻⁴	0.508	0.971
10 mM CaCl₂ + 0.64M NaCl	7.20 ± 0.07	2.36 * 10 ⁻⁴	0.473	0.977
0.67M NaCl	6.98 ± 0.04	3.74 * 10 ⁻⁵	0.330	0.985

As shown in the table, all linear regression coefficients (r^2) to the Freundlich equation for the different solutions are larger than 0.900, indicating that this equation successfully

describes the adsorption of phosphate on the gibbsite surface from the fluoride-free solutions. The adsorption capacity (K_F) values in Table 2.4.5 reflect the relative phosphate adsorption densities in each solution (Figure 2.4.3): Nanopure™ water > 10 mM CaCl₂ > 10 mM CaCl₂ + 0.64 M NaCl \cong seawater > 0.67 M NaCl.

To compare the K_F values for each solution on an even keel, the data were re-fit with an averaged $\beta = 0.44 \pm 0.06$ and K_F re-calculated for each adsorption density-final adsorbate concentration pair. Averaged K_F for each experimental solution are presented in Table 2.4.6. The calculated K_F values at equivalent β values reflect the order of adsorption capacities between the different solutions except for 0.67 M NaCl which is over-predicted, and seawater which is under-predicted.

Table 2.4.6 Re-calculated K_F values for each type of experimental solution with an average β of 0.44

	K_F
Nanopure™	$1.9 \pm 0.3 * 10^{-4}$
10 mM CaCl₂	$1.8 \pm 0.2 * 10^{-4}$
10 mM CaCl₂ + 0.64M NaCl	$1.6 \pm 0.2 * 10^{-4}$
0.67M NaCl	$1.4 \pm 0.2 * 10^{-4}$
Seawater	$1.3 \pm 0.2 * 10^{-4}$

2.4.4 Phosphate Adsorption in the Presence of Fluoride

With one exception (i.e., 10 mM CaCl₂ + 0.64 M NaCl), the presence of fluoride ions inhibits phosphate adsorption onto gibbsite from our experimental solutions (Figures 2.4.3 & 2.4.4). This phenomenon is most striking in Nanopure™ water where, in the absence of fluoride, phosphate adsorption is greatest, whereas in its presence adsorption is lowest.

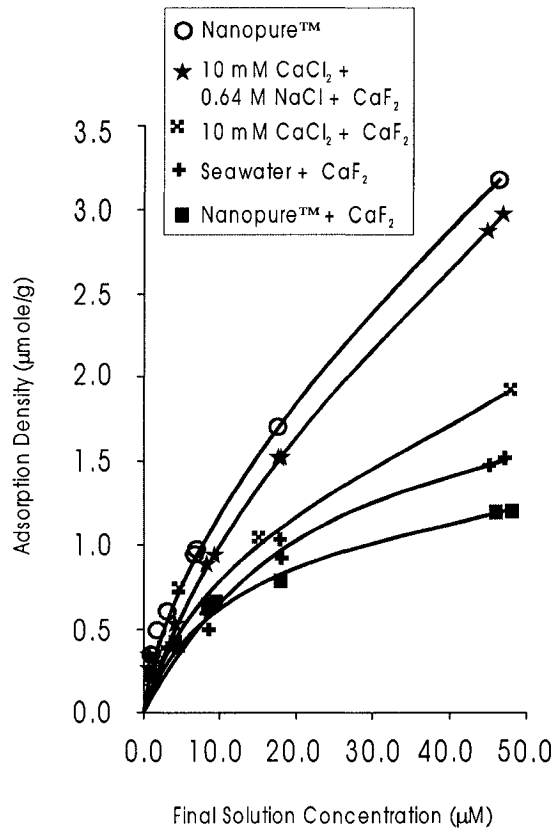


Figure 2.4.4 Adsorption Isotherms of phosphate onto gibbsite in F^- buffered solutions after 15 days @ $23 \pm 1^\circ C$ and $pH = 7.20 \pm 0.18$.

From Figure 2.4.4, the trend in adsorption capacities is; 10 mM $CaCl_2$ + 0.64 M $NaCl$ > 10 mM $CaCl_2$ > seawater > Nanopure™ water. The phosphate adsorption isotherms do not plateau over the range of concentrations investigated in this study, and, consequently were fit to the Freundlich equation. Freundlich equation parameters obtained from the fits are summarized in Table 2.4.7. All linear regression coefficients (r^2) for the different solutions are larger than 0.965. The values of K_F reported in Table 2.4.7 do not accurately reflect the relative affinities of phosphate for the gibbsite surface as observed in Figure 2.4.4 because the multiplicity factor, β , is highly variable between solutions.

Table 2.4.7 Freundlich parameters of phosphate isotherms in the fluoride-buffered solutions. The pH reported represents the average of all samples for each solution type.

	pH	K_F	β	r^2
10 mM CaCl₂ + 0.64M NaCl + F	7.17 ± 0.09	6.31 * 10 ⁻⁴	0.557	0.965
Seawater + F	7.34 ± 0.09	4.10 * 10 ⁻⁴	0.547	0.997
10 mM CaCl₂ + F	7.30 ± 0.08	1.26 * 10 ⁻⁴	0.427	0.975
Nanopure™ + F	7.00 ± 0.12	1.05 * 10 ⁻⁵	0.235	0.973

Re-calculating K_F values for each experimental solution at a fixed β proved futile because of the high variability of β values.

Fluoride concentrations in the fluoride-buffered phosphate adsorption solutions are assumed to be similar to those in the fluoride-buffered arsenate adsorption solutions but could not be determined accurately because of the strong interference of phosphate on the analysis (Hanocq and Molle, 1968).

2.5 Discussion

2.5.1 Effect of Ionic Strength on the Adsorption of Arsenate and Phosphate to Gibbsite

Surface complexation theory predicts that ionic strength in an indifferent electrolyte should decrease outer-sphere adsorption. In contrast, variations in ionic strength should not affect the adsorption behavior of species that form inner-sphere surface complexes (Stumm and Morgan, 1996). In the present study, both the arsenate and phosphate adsorption onto gibbsite are significantly reduced in a 0.67 M NaCl solution, an indifferent electrolyte with respect to the gibbsite surface, relative to Nanopure™ water. These observations may indicate that adsorption of both arsenate and phosphate on gibbsite at pH ~ 7.0 is not purely inner-sphere and that there is a certain degree of electrostatic interaction between the adsorbates and the gibbsite surface.

On the other hand, Criscenti and Sverjensky (1999) showed that adsorption behavior in solutions of variable salt concentrations is not definitive proof of outer-sphere complexation and that differences in adsorption at different salt concentrations may reflect the speciation of the adsorbate in solution, including formation of ion-pairs and ternary surface complexes with the background electrolyte. Millero (1982) and Millero and Schreiber (1982) provide values of the association constants for the ion-pairs $\text{NaH}_2\text{PO}_4^0$, NaHPO_4^- and NaPO_4^{2-} at $I = 0.7\text{M}$. In the phosphate-NaCl system, seven phosphate species are present: H_3PO_4 , H_2PO_4^- , HPO_4^{2-} , PO_4^{3-} , $\text{NaH}_2\text{PO}_4^0$, NaHPO_4^- and NaPO_4^{2-} . Among them, HPO_4^{2-} (55%) and NaHPO_4^- (35%) are predominant at the pH investigated in this study and approximately 40% of phosphate forms ion pair complexes with Na^+ . By analogy, and given the similarity of their chemical properties, arsenate

should also be paired with Na^+ . The data of Lowenthal et al. (1977), however, indicate that metal-arsenate ion pairs are less stable than metal-phosphate ion pairs. In contrast, metal-arsenate association constants found in Langmuir et al. (1999) extrapolated to $I = 0.7$ M using the PHREEQC v.2 computer code (Parkhurst and Appelo, 1999), indicate that metal-arsenate ion pairs are more stable than phosphate pairs, a result that is incompatible with estimates of the relative activity coefficients of both oxyanions in 0.7 M NaCl and seawater. In view of the conflicting literature data and for the remainder of the discussion, we will assume that association constants for arsenate are identical to those of phosphate for all our experimental solutions. Therefore, the formation of $\text{Na-AsO}_4/\text{Na-PO}_4$ pairs and their lack of affinity for the gibbsite surface may explain the decrease in adsorption upon the addition of 0.67 M NaCl to pure water.

2.5.2 Effect of Ca at its Seawater Concentration and Speciation on Arsenate and Phosphate Adsorption on Gibbsite in Fluoride-Free Solutions

The individual effect of Ca, at its seawater concentration (i.e. 10 mM) on arsenate and phosphate adsorption on gibbsite was studied at both low ($I = 0.03$ M) and high ($I = 0.67$ M) ionic strengths. It is clear from the arsenate and phosphate adsorption isotherms depicted in Figures 2.4.1 and 2.4.3 that the presence of Ca partially counteracts the decrease in adsorption caused by the increase in ionic strength or the presence of Na^+ in solution. The difference between adsorption isotherms in the low and high ionic strength solutions for both arsenate and phosphate are small, implying that the increase in adsorption reflects a strong affinity between Ca-PO_4 and Ca-AsO_4 and the gibbsite surface and this interaction is, at least, partly covalent.

Based on the stoichiometric aqueous association constants for phosphate ion-pairs of Millero and Schreiber (1982), and assuming that metal-arsenate ion pair association

constants are identical to those of phosphate (see section 2.3.1) allows for the determination of the dominant species present in the experimental solutions. In the PO₄-Ca and AsO₄-Ca systems at pH ≅ 7.0, CaHPO₄⁰/CaHAsO₄⁰ (50%) and HPO₄²⁻/HAsO₄²⁻ (35%) are the dominant species whereas in the PO₄-Ca-Na and AsO₄-Ca-Na systems at pH ≅ 7.0, HPO₄²⁻/HAsO₄²⁻ (65%), CaHPO₄⁰/CaHAsO₄⁰ (13%) and NaHPO₄⁻/NaHAsO₄⁻ (12%) are the dominant species.

Since there is a significant decrease in arsenate and phosphate adsorption in the 0.67 M NaCl solution relative to pure water, the NaHPO₄⁻ and NaHAsO₄⁻ ion pairs do not interact strongly with the gibbsite surface. On the other hand, the fact that Ca partially counteracts the decrease in adsorption caused by the increasing ionic strength suggests that CaHPO₄⁰ and CaHAsO₄⁰ ion pairs may form surface ternary complexes with gibbsite as proposed by Helyar et al. (1976a) for the same mineral and as suggested for the surface of goethite (Gao and Mucci, 2001, 2002).

At circum-neutral pH's, the proposed ternary surface complexes would form according to:

Ca-PO₄ system,



Ca-AsO₄ system,



The pH of all samples (arsenate and phosphate) was consistently lower and required raising after 48 and 72 hours in order to adjust it back to ~7.0. This observation is consistent with the proposed surface reactions above, all of which lead to the release of protons from the surface.

2.5.3 Arsenate and Phosphate Adsorption on Gibbsite in Fluoride-Free Artificial Seawater

Arsenate (Fig. 2.4.2) and phosphate (Fig 2.4.3) adsorption in fluoride-free artificial seawater is slightly less than in the 10 mM CaCl₂ and 10 mM CaCl₂ + 0.64 M NaCl solutions but significantly greater than in 0.67 M NaCl. Decreased adsorption in F⁻-free seawater relative to the 10 mM CaCl₂ + 0.64 M NaCl solution must be related to the influence of other major seawater ions other than Cl and Na since both solutions are at equivalent ionic strengths. Using the stoichiometric, aqueous association constants of Millero (1982) and Millero and Schreiber (1982), and assuming that metal-arsenate ion pair association constants are identical to those of phosphate (see section 2.5.1), we determined that MgHPO₄⁰/MgHAsO₄⁰ (40%), HPO₄²⁻/HAsO₄²⁻ (25%), NaHPO₄⁰/NaHAsO₄⁰ (15%) and CaHPO₄⁰/CaHAsO₄⁰ (10%) are the dominant phosphate and arsenate species in the F⁻-free seawater solution. The relative amounts of these species suggest that the increase in adsorption in F⁻-free artificial seawater relative to 0.67 M NaCl reflects a stronger affinity of Ca based ternary surface complexes for the gibbsite surface as opposed to Na based complexes even if Na ion pairs are more abundant in solution. The decrease in adsorption in F⁻-free seawater relative to the simpler salt solutions (high and low ionic strengths) may result from the decrease in Ca-adsorbate pairs available to form ternary complexes with the gibbsite surface because of competition from other ions such as Mg to form ion pairs with the oxyanions.

Alternatively, the decrease may also result from competition for surface sites by seawater anions such as CO_3^{2-} and B(OH)_4^- . Goldberg et al. (1993) reported that boron (borate) forms a strong-inner sphere complex at the gibbsite surface and, thus, the presence of borate in the F^- -free seawater solution may compete with arsenate and phosphate for adsorption sites on the gibbsite surface. On the other hand, the presence of SO_4^{2-} and HCO_3^- is not believed to affect arsenate and phosphate adsorption. Sulfate reduces arsenate adsorption on α -alumina only at low pH (i.e., $\text{pH} < 6$; Xu et al., 1988) and Helyar et al. (1976b) reported that bicarbonate at a lower concentration than seawater has no measurable effect on phosphate adsorption on gibbsite. Additional studies will be required to verify these hypotheses and elucidate the adsorption behavior in a complex electrolyte such as seawater.

2.5.4 Effect of the Fluoride Ion on the Adsorption of Arsenate on Gibbsite

The increase in arsenate adsorption in the presence of fluoride ions relative to Nanopure™ water seen in Figure 2.4.2 is striking. Hingston et al. (1972 and 1981) and Farrah et al. (1987) showed that fluoride strongly adsorbs to gibbsite in dilute solutions and Choi and Chen (1979) and Hao and Huang (1986) reported that the removal of wastewater fluoride by alumina is unaffected by salinity. Crecelius et al. (1986) through both computer modeling (thermodynamic data of Ball et al., (1980)) and chromatographic studies predict that at least 10% of the total As(V) occurs as HAsO_3F^- at the fluoride concentrations and pH values investigated in this study. We suggest that HAsO_3F^- pairs which make up to 10% of the As(V) species present in the F^- -buffered experimental solutions, share a similar affinity to F^- for the gibbsite surface, and, thus, the formation of arsenate-fluoride complexes and their adsorption as ternary complexes to

gibbsite may account for the significant increase in arsenate adsorption in the presence of fluoride observed in this study.

The proposed ternary surface complexes would form as follows:

F-AsO₄ system,



The stoichiometry of these reactions is consistent with the observation that the pH of all our experimental solutions had to be adjusted upwards to pH 7.0 after 48 and 72 hours of equilibration.

Arsenate adsorption in the presence of fluoride is greatest in the 10 mM CaCl₂ solution followed by 10 mM CaCl₂ + 0.64 M NaCl, seawater and Nanopure™ water, the same trend as in the fluoride-free solutions. We attribute this trend to the formation of both arsenate-fluoride and arsenate-calcium ternary surface complexes.

2.5.5 Effect of the Fluoride Ion on the Adsorption of Phosphate on Gibbsite

With one exception (i.e. 10 mM CaCl₂ + 0.64 M NaCl), the presence of fluoride ions inhibits phosphate adsorption onto gibbsite (Fig. 2.4.4) in accordance with the findings of Kuo and Lotse (1974). This phenomenon is most striking in Nanopure™ water where, in the absence of fluoride, phosphate adsorption on gibbsite is greatest whereas in its presence it displays the lowest adsorption density. We attribute the decrease of phosphate adsorption to the adsorption of fluoride on the gibbsite surface, out-competing phosphate species. In contrast to arsenate-fluoride complexes, the formation of phosphate-fluoride complexes are undocumented in the literature. Nonetheless, given their similar chemical properties it is fair to assume that they exist in ratios similar to

arsenate-fluoride complexes but our results suggest that these do not share a high affinity for the gibbsite surface as does F^- and the arsenate-fluoride pairs.

2.5.6 Comparison Between Arsenate and Phosphate Adsorption

Phosphate adsorption density on gibbsite is greater than arsenate in the fluoride-free solutions (Figures 2.4.1 and 2.4.3). These observations are consistent with those of Manning and Goldberg (1996), Okazaki et al. (1989) and Hingston et al. (1971), all of whom have reported greater adsorption densities for phosphate relative to arsenate on gibbsite and α -alumina. Hingston (1981) suggests that it is related to steric (size) effects although it may reflect a greater chemical affinity (covalency) between phosphate and the gibbsite surface, the two are not mutually exclusive.

Regardless of the slight adsorption density difference between the adsorbates in equivalent fluoride-free solutions, both respond similarly to the addition of Ca even in high ionic strength solutions (i.e., $I = 0.67M$). We attribute this phenomenon to the formation of ternary surface complexes between the adsorbates, Ca and the gibbsite surface (see section 2.3.2).

Arsenate adsorption density is an order of magnitude greater than phosphate adsorption at equivalent fluoride concentrations. The difference is ascribed to the formation of arsenate-fluoride complexes that have a strong affinity for the gibbsite surface and the absence of a similar phosphate-fluoride species or the lack of affinity of this species for the gibbsite surface.

2.6 Conclusions

The primary objective of this study was to determine how the adsorption capacity of gibbsite for arsenate and phosphate varies as a function of ionic strength and composition of the solution with special attention to the effect of the fluoride ion. Ultimately this was to simulate the behavior of the adsorbent/adsorbate relationship during estuarine mixing.

The greatest adsorbate adsorption densities measured in the fluoride-free solutions occur in Nanopure™ water, whereas the lowest adsorbate adsorption densities measured in the fluoride-free solutions occur in 0.67 M NaCl. This implies that adsorption of both arsenate and phosphate on gibbsite at $\text{pH} \cong 7.0$ is either not purely inner-sphere, in other words, there is a certain degree of electrostatic interaction between the adsorbates and the gibbsite surface, or the formation of ion pairs with the background electrolyte (i.e., $\text{NaPO}_4/\text{NaAsO}_4$), stabilizes the adsorbates in solution.

The presence of Ca at its seawater concentration (i.e. 10 mM) partially counteracts the decrease in adsorption of both adsorbates caused by the increase in ionic strength. This increase is ascribed to the formation of adsorbate/Ca aqueous complexes that have a strong affinity for, and form ternary complexes, with the gibbsite surface.

Arsenate and phosphate adsorption in fluoride-free artificial seawater is slightly less than in the 10 mM CaCl_2 and 10 mM $\text{CaCl}_2 + 0.64 \text{ M NaCl}$ solutions but significantly greater than in 0.67 M NaCl. We propose that Ca ternary complexes may also account for the increased adsorption relative to 0.67 M NaCl. Magnesium-adsorbate ion pairs are more abundant in seawater than are Ca-adsorbate ion pairs and, thus, we hypothesize that Mg ion pairs may not form as stable ternary complex with the gibbsite surface. In the

absence of data from a Na-Mg-Cl system this interpretation remains speculative. The presence of borate which has a strong affinity for the gibbsite surface may compete with the arsenate and phosphate and may account for the decrease in their adsorption in seawater relative to the 10 mM CaCl₂ and 10 mM CaCl₂ + 0.64 M NaCl solutions.

There is a striking difference between arsenate and phosphate adsorption on gibbsite in the presence of fluoride ions. Arsenate adsorption in each of our experimental solutions increases by one order of magnitude in the presence of fluoride whereas, with one exception (10 mM CaCl₂ + 0.64 M NaCl), the presence of fluoride decreases the adsorption of phosphate. We propose that the formation of arsenate-fluoride aqueous complexes and their adsorption to the gibbsite surface as ternary surface complexes may account for the increase in arsenate adsorption in the presence of fluoride. The absence of a similar behavior with phosphate may reflect the lack of affinity or absence of phosphate-fluoride complexes.

The results of this study have interesting implications with respect to the fate of arsenate and phosphate during estuarine mixing. The increase in ionic strength experienced by a gibbsite particle as it is carried by river waters through an estuary will induce desorption of both arsenate and phosphate. At the same time, the concentration of Ca²⁺ (i.e., [Ca²⁺]_{RW} = 0.74 mM, [Ca²⁺]_{SW} = 10.28 mM @ S = 35) will increase and partially counteract the effect of the increasing ionic strength. Finally, a concurrent increase of the concentration of F⁻ (i.e., [F⁻]_{RW} = 5.0 μM, [F⁻] = 70.0 μM @ S = 35) will promote arsenate adsorption but inhibit phosphate adsorption. The combination of factors will likely result in some desorption of phosphate and very little desorption of

arsenate. It is also possible that the release of some phosphate will liberate adsorption sites to be occupied by arsenate.

Arsenate and phosphorus are both group V elements and, thus, are expected have similar chemical properties and display similar geochemical behaviors. This study demonstrates that in the presence of the fluoride ion at seawater concentrations, arsenate adsorption is one order of magnitude greater than phosphate adsorption on gibbsite. Therefore, arsenate and phosphate are de-coupled from each other with respect to adsorption on gibbsite in the presence of fluoride at seawater concentrations.

In natural estuarine environments there are often a lot more detrital and authigenic iron oxides (i.e., Millward et al., 1987; Lucotte and d'Anglejan, 1988; Mucci et al., 2000; Saulnier and Mucci, 2000; Gao and Mucci, 2002) than aluminum oxide particles and numerous studies have shown that they are strong scavengers of PO_4 and AsO_4 (Hingston et al., 1968; Pierce and Moore, 1982; Mucci et al., 2000). Adsorption of these oxyanions by iron oxides does not appear to vary significantly as the solution composition is varied so that whatever fraction of phosphate is desorbed from an aluminum oxide upon mixing of river water with seawater will be rapidly adsorbed by iron oxides which are ubiquitous in these environments.

2.7 References

- Abdullah, M. I., Shiyu, Z. and Mosgren, K., 1995. Arsenic and selenium species in the oxic and anoxic waters of the Oslofjord, Norway. *Mar. Pol. Bull.*, 31: 116-126.
- Aggett, J. and Aspell, A. C., 1976. The determination of arsenic (III) and total arsenic by atomic adsorption spectroscopy. *Analyst*, 101: 341-347.
- Anderson, L.C.D. and Bruland, K.W., 1991. Biogeochemistry of arsenic in natural waters: The importance of methylated species. *Environ. Sci. Technol.*, 25: 420-427.
- Anderson, M. A., Ferguson, J. F. and Gavis, J., 1976. Arsenate adsorption on amorphous aluminum hydroxide. *J. Colloid Interface Sci.*, 54: 391-399.
- Anderson, M. A. and Malotky, D. T., 1979. The adsorption of protolyzable anions on hydrous oxides at the isoelectric pH. *J. Colloid Interface Sci.*, 72: 413-427.
- Andreae, M. O., 1978. Distribution and speciation of arsenic in natural waters and some marine algae. *Deep Sea Res.*, 25: 391-402.
- Bache, B. W., 1964. Aluminum and iron phosphate studies relating to soils II Reactions between phosphate and hydrous oxides. *J. Soil Sci.*, 15: 110-116.
- Ball, J.W., Jenne, E.A., and Nordstrom, D.K., 1980. Additional and revised thermochemical data and computer code for WATEQ. A computerized chemical model for trace and major element speciation and mineral equilibria of natural waters. U.S. Geol. Survey Water Res Invest., 78-116.
- Belzile, N. and Lebel, J., 1986. Capture of arsenic by pyrite in near-shore marine sediment. *Chem. Geol.*, 54: 279-281.
- Bower, C.A. and Hatcher, J.T., 1967. Adsorption of fluoride by soils and minerals. *Soil Sci.*, 103: 151-154.
- Boyle, R. W. and Jonasson, I. R., 1973. The geochemistry of arsenic and its use as an indicator element in geochemical prospecting. *J. Geochem. Exploration*, 2: 251-296.
- Chen, Y. R., Butler, J.N. and Stumm, W., 1972. Adsorption of phosphate on alumina and kaolinite from dilute aqueous solutions. *J. Colloid Interface Sci.*, 43: 421-436.
- Choi, W. W. and Chen, K. Y., 1979. The removal of fluoride from waters by adsorption. *J. Am. Water Works Assoc.*, 71: 562-570.
- Crecelius, E. A., Bloom, N. S., Cowan C. E. and Jenne E. A., 1986. Speciation of selenium and arsenic in natural waters and sediments, Vol. 2. Electrical Power Research Institute, Research Project 2020-2, California.

- Criscenti, L.J. and Sverjensky, D.A., 1999. The role of electrolyte ions (ClO_4^- , NO_3^- , and Cl^-) in divalent metal (M^{2+}) adsorption on oxide and hydroxide surfaces in salt solution. *Am. J. Sci.*, 299: 828-899.
- Dougan, W. K. and Wilson, A. L., 1974. The absorptiometric determination of aluminum in water. A comparison of some chromogenic reagents and the development of an improved method. *Analyst*, 99 413-430.
- Elrashidi, M.A. and Lindsay, W.L., 1986. Chemical equilibria of fluorine in soils: A theoretical development. *Soil Sci.*, 141: 275-280.
- Farrah, H., Slavek, J. and Pickering, W. F., 1987. Fluoride interactions with hydrous aluminum oxides and alumina. *Austral. J. Soil Res.*, 25: 55-69.
- Fitzpatrick, A. J., 1998. The adsorption of arsenate and phosphate on gibbsite from artificial seawater. M.Sc. Thesis, McGill University.
- Fowler, B.A., Ishiniski, N., Tsuchiya, K. and Vahter, M., 1979. Arsenic. In: L. Briberg (Editor), *Handbook on the Toxicology of Metals*. Elsevier-North-Holland Biomedical Press, pp. 293-319.
- Gao, Y. and Mucci, A., 2001. Acid base reactions, phosphate and arsenate complexation, and their competitive adsorption at the surface of goethite in 0.7 M NaCl solution. *Geochim. Cosmochim. Acta*, 65: 2361-2378.
- Gao, Y. and Mucci, A., 2002. Individual and competitive adsorption of phosphate and arsenate on goethite in artificial seawater. *Chem. Geol.* In Press.
- Goldberg, S., Davis J. A., and Hem, J. D., 1996. The surface chemistry of aluminum oxides and hydroxides. In: G. Sposito (Editor), *The Environmental Chemistry of Aluminum*, CRC Press, Florida, pp. 271-331.
- Goldberg, S., Foster, H. S., and Heick E. L., 1993. Boron adsorption mechanisms on oxides, clay minerals, and soils inferred from ionic strength effects. *Soil Sci. Soc. Am. J.*, 57: 704-708.
- Gomez, E., Durillon, G.E., and Picot, B., 1999. Phosphate adsorption and release from sediments of brackish lagoons; pH, O_2 and loading influence. *Wat. Res.*, 10: 2437-2447.
- Halter, W.E. and Pfeifer, H.R., 2001. Arsenic (V) adsorption onto $\alpha\text{-Al}_2\text{O}_3$ between 25 and 70°C. *Appl. Geochem.*, 16: 793-802.
- Hanocq, M. and Molle, L., 1968. Dosage par spectrophotometrie dans l'ultraviolet de l'ion fluorure a l'aide des chelates. *Analytica Chimica Acta.*, 42: 349-356.

- Hao, O. J. and Huang, C. P., 1986. Adsorption characteristics of fluoride onto hydrous alumina. *J. Environ. Engineer.*, 112: 1054-1069.
- Helyar, K. R., Munns, D. N. and Burau, R. G., 1976a. Adsorption of phosphate by gibbsite II Formation of a surface complex involving divalent cations. *J. Soil Sci.*, 27: 315-323.
- Helyar, K. R., Munns, D. N. and Burau, R. G., 1976b. Adsorption of phosphate by gibbsite. I. Effects of neutral chloride salts of calcium, magnesium, sodium, and potassium. *J. Soil Sci.*, 27: 307-314.
- Hingston, F. J., 1981. A review of anion adsorption. In: M. A. Anderson and A. J. Rubin (Editors) *Adsorption of Inorganics at Solid-Liquid Interface*. Ann Arbor Science, Ann Arbor, Michigan, pp. 51-90.
- Hingston, F. J., Atkinson, R.J., Posner, A. M. and Quirk, J. P., 1968. Specific adsorption of anions on goethite. *9th Int. Cong. Soil Sci. Trans.*, 1: 669-678.
- Hingston, F. J., Posner, A. M. and Quirk, J. P., 1971. Competitive adsorption of negatively charged ligands on oxide surfaces. *Disc. Faraday Soc.*, 52: 334-342.
- Hingston, F. J., Posner, A. M. and Quirk, J. P., 1972. Anion adsorption by goethite and gibbsite. I. The role of the proton in determining adsorption envelopes. *J. Soil Sci.*, 23: 177-192.
- Huang, C. P., 1975. Adsorption of phosphate at the hydrous γ -Al₂O₃-electrolyte Interface. *J. Colloid Interface Sci.*, 53: 178-186.
- Huang, C. P. and Stumm, W., 1973. Specific adsorption of cations on hydrous α -Al₂O₃. *J. Colloid Interface Sci.* 22, 231-259.
- Jambor, J.L., Sabina, A.P., Ramik, R.A. and Sturman, B.D., 1990. A fluorine-bearing gibbsite-like mineral from the Francon quarry, Montreal, Quebec. *Can. Min.*, 28: 147-159.
- Kester, D. R., Duedall, I. W., Connor, D. N. and Pytkowicz, R. M., 1969. Preparation of artificial seawater. *Limnol. Oceanogr.* 12: 176-179.
- Kinniburgh, D. G., 1986. General purpose adsorption isotherms. *Environ. Sci. Technol.*, 20: 895-904.
- Koroleff, F., 1976. Determination of phosphorous. In: K. Grasshoff (Editor), *Methods of Seawater Analysis*. Verlag Chemie, New York, 117-126.
- Kuo, S. and Lotse, E. G., 1974. Kinetics of phosphate adsorption and desorption by hematite and gibbsite. *Soil Sci.*, 116: 400-406.

- Kyle, J. H., Posner, A. M. and Quirk, J. P., 1975. Kinetics of isotopic exchange of phosphate adsorbed on gibbsite. *J. Soil Sci.*, 26: 32-43.
- Langmuir, D., 1997. *Aqueous Environmental Geochemistry*. Prentice-Hall Canada Inc. Toronto.
- Langmuir, D., Mahoney, J., MacDonald, A. and Rowson, J., 1999. Predicting arsenic concentrations in the porewaters of buried uranium mill tailings. *Geochim. Cosmochim. Acta*, 63: 3379-3394.
- Lantzy, R. J. and Mackenzie, F. T., 1994. Tentative model of global oceanic cycling behaviour of arsenic. In: T. C. G. Hutchinson, C.A. and K. Meema (Editors), *Global Perspectives on Lead, Mercury and Cadmium Cycling in the Environment*. John Wiley Eastern Ltd. Publishers, New Delhi, India, pp. 95-114.
- Livesey, N. T. and Huang, P. M., 1981. Adsorption of arsenate by soils and its relation to selected chemical properties and anions. *Soil Sci.*, 131: 88-94.
- Lowenthal, D. H., Pilson, M. E. Q. and Byrne, R. H., 1977. The determination of the apparent dissociation constants of arsenic acid in seawater. *J. Marine Res.*, 35: 653-669.
- Lucotte, M. and d'Anglejan, B., 1988. Processes controlling phosphate adsorption by iron hydroxides in estuaries. *Chem. Geol.*, 67: 75-83.
- Manning, B. A. and Goldberg, S., 1996. Modeling competitive adsorption of arsenate with phosphate and molybdate on oxide minerals. *Soil Sci. Soc. Am. J.*, 60: 121-131.
- Massee, R., Maessen, F. J. and De Goeij, J. J. M., 1981. Losses of silver, arsenic, cadmium, selenium and zinc traces from distilled water and artificial seawater on various container surfaces. *Anal. Chim. Acta*, 127: 181-193.
- May, H.M., Helmke, P.A. and Jackson, M.L., 1979. Gibbsite solubility and thermodynamic properties of hydroxy-aluminum ions in aqueous solution at 25°C. *Geochim. Cosmochim. Acta*, 43: 861-868.
- Millero, F.J., 1982. Use of models to determine ionic interactions in natural waters. *Thal. J.*, 18: 253-291.
- Millero, F.J. and Schreiber, D.R., 1982. Use of the ion pairing model to estimate activity coefficients of the ionic components of natural waters. *Amer. J. Sci.*, 282: 1508-1540.
- Millero, F.J., Hershey, J.P., Fernandez, M., 1987. The pK^* of $TRISH^+$ in Na-K-Mg-Ca-Cl-SO₄ brines -pH scales. *Geochim. Cosmochim. Acta*, 51: 707-711.
- Millero, F.J., Zhang, J.Z., Fiol, S., Sotolongo, S., Roy, R.N., Lee, K., Mane, S., 1993. The use of buffers to measure the pH of seawater. *Mar. Chem.*, 44: 143-152.

Millward, G.E., Marsh, J.G., Crosby, S.A., Whitefield, M., Langston, W.J. and O'Neil, P., 1987. Adsorption kinetics of waste generated arsenate and phosphate at the iron oxyhydroxide-seawater interface. In: T.P. O'connor, W.V. Burt and I.W. Duedall (Editors), *Oceanic Process in Marine Pollution. Volume 2: Physiochemical process and wastes in the ocean.* Robert E. Krieger, Malabar, Florida. pp.133-143.

Mucci, A., Richard, L.-F., Lucotte, M. and Guignard, C., 2000. The differential geochemical behaviour of arsenic and phosphorus in the water column and sediments of the Saguenay Fjord Estuary, Canada. *Aquat. Geochem.*, 6: 293-324.

Muljadi, D., Posner, A. M. and Quirk, J. P., 1966. The mechanism of phosphate adsorption by kaolinite, gibbsite and pseudoboehmite. I. The isotherms and the effect of pH on adsorption. *J. Soil Sci.*, 17: 212-229.

NRCC, 1978. Effects of arsenic in the Canadian environment. National Research Council of Canada Associate Committee On Scientific Criteria For Environmental Quality.

Okazaki, M., Sakaidani, K., Saigusa, T. and Sakaida, N., 1989. Ligand exchange of oxyanions on synthetic hydrated oxides of iron and aluminum. *Soil Sci. Plant Nutrit.*, 35: 337-346.

Parfitt, R. L., Fraser, A. R., Russell, J. D. and Farmer, V. C., 1977. Adsorption of hydrous oxides. II. Oxalate, benzoate, and phosphate on gibbsite. *J. Soil Sci.*, 26: 40-47.

Parkhurst, D.L. and Appelo, C.A.J., 1999. User's guide to PHREEQC (version 2). A computer program for speciation, batch-reaction, one-dimensional transport, and inverse geochemical calculations. U.S. Geological Survey Water-Resources Investigations Report 99-4259.

Pierce, M.L. and Moore, C.B., 1982. Adsorption of arsenite and arsenate on amorphous iron hydroxide. *Water Res.*, 16: 1247-1253.

Planas, D. and Healy, F. P., 1978. Effects of arsenate on growth and phosphorus metabolism of phytoplankton. *J. Phycol.*, 14: 337-341.

Riedel, G. F., 1993. The annual cycle of arsenic in a temperate estuary. *Estuaries* 16: 533-540.

Roberson, C. E. and Hem, J. D., 1969. Solubility of aluminum in the presence of hydroxide, fluoride and sulfate. USGS Paper 1827-C.

Russell, J. D., Parfitt, R. L., Fraser, A. R. and Farmer, V. C., 1974. Surface structures of gibbsite, goethite and phosphated goethite. *Nature*, 248: 220-221.

Sadiq, M., 1992. Toxic metal chemistry in marine environments. Marcel Dekker, New York.

- Sanders, J.G. and Windom, H.L., 1980. The uptake and reduction of arsenic species by marine algae. *Estuar. Coast. Mar. Sci.*, 10: 555-567.
- Sanders, J.G., 1983. Role of marine phytoplankton in determining the chemical speciation and biogeochemical cycling of arsenic. *Can. J. Fish. Aquat. Sci.*, 40: 192-196.
- Sanjuan, B. and Michard, G., 1987. Aluminum hydroxide solubility in aqueous solutions containing fluoride ions at 50°C. *Geochim. Cosmochim. Acta*, 51: 1823-1831.
- Saulnier, I. and Mucci, A., 2000. Trace metal remobilization following the resuspension of estuarine sediments: Saguenay Fjord, Canada. *Appl. Geochem.*, 15:191-210.
- Seyler, P. and Martin, J.M., 1990. Distribution of arsenite and total dissolved arsenic in major French estuaries: dependence on biogeochemical processes and anthropogenic inputs. *Mar. Chem.*, 29: 277-294.
- Smedley, P.L. and Kinniburgh, D.G., 2002. A review of the source, behaviour and distribution of arsenic in natural waters. *Appl. Geochem.*, 17:517-568.
- Stryer, L., 1988. *Biochemistry*. W.H. Freeman, New York.
- Stumm, W. and Morgan, J.J., 1996. *Aquatic Chemistry: Chemical Equilibria and Rates in Natural Waters*. Wiley-Interscience, New York.
- Sullivan, K.A. and Aller, R.C., 1996. Diagenetic cycling of arsenic in Amazon shelf sediments. *Geochim. Cosmochim. Acta*, 60: 1465-1477.
- Sundby, B., Gobeil, C., Silverberg, N. and Mucci, A., 1992. The phosphorous cycle in coastal marine sediments. *Limnol. Oceanogr.*, 37: 1129-1145.
- van Riemsdijk, W. H. and Lijklema, J., 1980. Reaction of phosphate with gibbsite [Al(OH)₃] beyond the adsorption maximum. *J. Colloid Interface Sci.*, 76: 55-66.
- Vieth, J. A. and Sposito, G., 1977. On the use of the Langmuir equation in the interpretation of "adsorption" phenomena. *Soil Sci. Soc. Am. J.*, 41: 697-702.
- Violante, A., Colombo, C., and Buondonno, A., 1991. Competitive adsorption of phosphate and oxalate by aluminum oxides. *Soil Sci. Soc. Am. J.*, 55: 65-70.
- Waslenchuk, D.G., 1978. The budget and geochemistry of arsenic in a continental shelf environment. *Mar. Chem.*, 7: 39-52.
- Widerlund, A. and Ingri, J., 1995. Early diagenesis of arsenic in sediments of the Kalix River estuary, northern Sweden. *Chem. Geol.*, 125: 185-196.

Xu, H., Allard B. and Grimvall, A., 1988. Influence of pH and organic substance on the adsorption of As(V) on geological materials. *Water Air Soil Poll.*, 40: 293-305.

Xu, H., Allard B. and Grimvall A., 1991. Effects of acidification and natural organic materials on the mobility of arsenic in the environment. *Water Air Soil Poll.*, 57-58: 269-278.

Yao, W. and Millero, F.J., 1996. Adsorption of phosphate on manganese dioxide in seawater. *Environ. Sci. Technol.*, 35: 536-541.

Wu, C.H., Kuo, C.Y., Lin, C.F. and Lo, S.L., 2002. Modelling competitive adsorption of molybdate, sulfate, selenate, and selenite using a Freundlich-type multi-component isotherm. *Chemosphere*, 47: 283-292.

2.8 Appendix

Appendix 2.8.1 Arsenate adsorption to gibbsite for each F-free experimental solution. Aluminum concentrations included where measured.

Solution Type	pH	Final [As]		Final [Al]
		μM ($\pm 5\%$)	Γ $\mu\text{mol/g}$ ($\pm 5\%$)	μM ($\pm 10\%$)
Nanopure™	7.23	1.72	0.248	0.89
	7.18	4.58	0.395	
	7.19	9.59	0.892	
	7.24	17.0	2.660	1.44
	7.35	47.4	2.580	1.14
10 mM CaCl₂	6.94	0.89	0.111	1.36
	7.02	4.71	0.352	
	7.10	9.16	0.916	
	7.05	19.0	1.280	1.22
	7.19	46.5	1.850	1.42
10 mM CaCl₂ + 0.64 M NaCl	7.25	0.73	0.235	1.63
	7.12	1.73	0.263	
	7.18	4.22	0.744	
	7.22	8.88	1.130	
	7.38	18.8	1.440	1.92
	7.24	46.6	2.170	2.11
Seawater	7.25	0.91	0.009	0.93
	7.17	1.90	0.129	
	7.28	4.55	0.478	
	7.14	9.34	0.771	
	7.17	19.1	1.200	1.11
	7.19	47.0	1.760	1.52
0.67 M NaCl	7.23	0.81	0.164	1.41
	7.09	1.70	0.263	
	7.22	4.58	0.392	
	7.22	9.47	0.526	
	7.29	19.1	0.932	1.86
	7.29	48.7	1.560	1.42

Appendix 2.8.2 Arsenate adsorption to gibbsite for each F⁻-buffered experimental solution. Aluminum concentrations included where measured.

Solution Type	pH	Final [As]	Γ $\mu\text{mol/g}$ ($\pm 5\%$)	Final [F]	Final [Al]
		μM ($\pm 5\%$)		μM ($\pm 2\%$)	μM ($\pm 10\%$)
Nanopure™ + F⁻	6.68	1.06	0.07	61.0	1.12
	6.70	2.20	0.60	76.0	
	6.87	5.32	0.83	71.0	
	7.21	8.83	2.14	61.5	
	7.02	20.0	2.92	58.0	1.25
	7.33	48.7	6.68	52.6	1.32
10 mM CaCl₂ + F⁻	6.84	0.97	0.05	45.0	1.25
	6.94	1.92	0.19	34.0	
	6.97	4.27	0.90	45.0	
	7.02	5.76	3.62	50.0	
	7.07	13.0	6.04	66.0	1.13
	7.12	34.0	14.10	68.0	1.24
10 mM CaCl₂ + 0.64 M NaCl + F⁻	6.92	1.73	0.26	26.8	1.77
	6.88	4.75	0.83	31.6	
	6.90	8.68	1.98	42.0	
	6.88	14.5	4.85	74.0	2.33
	7.02	38.0	10.80	35.2	3.42
Seawater + F⁻	7.19	1.86	0.16	120.6	0.84
	7.01	4.69	0.37	105.4	
	7.02	10.3	0.87	121.8	
	7.04	17.5	2.51	105.3	3.81
	7.02	40.7	8.57	126.4	2.69

Appendix 2.8.3 Phosphate adsorption to gibbsite for each experimental solution

Solution Type	pH	Final [P]		Solution Type	pH	Final [P]	
		μM ($\pm 10\%$)	$\Gamma \mu\text{mol/g}$ ($\pm 10\%$)			μM ($\pm 10\%$)	$\Gamma \mu\text{mol/g}$ ($\pm 10\%$)
Nanopure™	6.88	4.00	0.68	Nanopure™ + F⁻	7.11	4.10	0.59
	7.02	8.67	0.82		7.12	8.80	0.70
	7.24	46.0	3.19		6.77	0.52	0.38
	7.12	1.33	0.54		6.80	1.49	0.40
	6.90	4.00	0.68		7.01	9.10	0.72
	7.22	8.85	0.92		6.88	18.0	0.80
	7.08	18.3	1.37		7.02	48.2	1.04
10 mM CaCl₂	6.90	0.85	0.35	10 mM CaCl₂ + F⁻	7.21	0.49	0.25
	6.90	18.7	1.61		7.30	1.18	0.36
	7.10	47.0	2.34		7.40	4.06	0.75
	7.00	3.99	0.73		7.33	9.08	0.74
	7.10	8.95	0.84		7.44	18.7	1.15
	7.12	18.5	1.63		7.27	47.9	1.92
	7.20	48.3	2.43				
10 mM CaCl₂ + 0.64 M NaCl	7.20	0.57	0.29	10 mM CaCl₂ + 0.64 M NaCl + F⁻	7.20	0.45	0.25
	7.25	1.55	0.36		7.20	1.50	0.29
	7.20	4.24	0.61		7.17	8.93	0.85
	7.26	8.78	0.98		7.07	18.2	1.44
	7.24	4.07	0.74		7.00	43.3	2.65
	7.23	8.79	0.97		7.22	0.70	0.26
	7.17	18.2	1.45		7.28	4.34	0.53
	7.04	47.4	2.06		7.15	8.92	0.87
Seawater	7.30	0.72	0.224	7.29	18.2	1.47	
	7.30	4.43	0.456	7.14	46.3	2.98	
	7.45	4.04	0.574	Seawater + F⁻	7.40	4.54	0.37
	7.43	8.77	0.938		7.40	9.32	0.79
	7.48	17.6	1.13		7.40	18.8	1.06
	7.30	45.3	1.75		7.40	48.1	1.65
0.67 M NaCl	7.17	0.60	0.32	7.34	8.78	0.927	
	7.01	1.45	0.44	7.40	17.6	1.15	
	7.17	4.10	0.72	7.30	45.5	1.62	
	7.06	9.00	0.80				
	7.05	19.1	0.77				
	7.12	48.3	1.04				

CHAPTER 3

The Influence of Ionic Strength and Solution Composition on the Solubility of Fluorite at 25 °C and One Atmosphere Total Pressure.

Forward

In Chapter 2 we investigated the adsorption capacity and affinity of gibbsite for arsenate and phosphate in solutions of varying ionic strength and composition, including seawater in the absence and presence of the fluoride ion. Particular attention was paid to the fluoride ion because of its status as a major seawater constituent and its known affinity for the gibbsite surface. In order to maintain the fluoride ion activity constant in our experimental solutions, a fluorite crystal was added to the reactional systems.

We searched the literature to find the stoichiometric solubility of fluorite in seawater and, hence, derive the equilibrium fluoride concentration in this solution and discovered that it has never been measured. Alternatively, the equilibrium fluoride concentration can be estimated from the thermodynamic solubility, K_{sp}^0 , of fluorite at 25 °C and one atmosphere pressure and estimates of the Ca^{2+} and F^- ion activity ($\gamma_{\text{Ca}^{2+}}$ and γ_{F^-}) coefficients. The $\gamma_{\text{Ca}^{2+}}$ estimates are well constrained in seawater, but the only estimate of the γ_{F^-} in seawater was derived from measurements of the apparent dissociation constant of hydrofluoric acid (HF), under conditions (i.e. acidic pH) that are far from realistic natural conditions. Furthermore, a survey of the literature revealed that published values of the K_{sp}^0 (fluorite) vary by one order of magnitude.

Therefore, in Chapter 3, fluorite equilibration experiments were carried out in a variety of experimental solutions of known compositions at 25 °C and 1 atmosphere total pressure to determine the effect of ionic strength and the potential co-precipitation of a seawater constituent on the solubility of fluorite.

**The Influence of Ionic Strength and Solution Composition on the
Solubility of Fluorite at 25 °C and One Atmosphere Total Pressure**

Alain Garand and Alfonso Mucci

Department of Earth and Planetary Sciences

McGill University

3450 University Street

Montreal, Qc H3A 2A7

Canada

Fax: (514) 398-4680

Email: alm@eps.mcgill.ca

To be Submitted to Marine Chemistry

3.1 Abstract

The stoichiometric solubility of fluorite was measured in a variety of aqueous solutions, including artificial seawater at 25⁰C and 1 atmosphere total pressure in order to determine the effect of ionic strength and the potential co-precipitation of seawater constituents on the equilibrium ion concentration product.

The ion concentration products (ICP = [Ca²⁺][F⁻]²) measured after 32 weeks of equilibration become invariant or converge to constant values. The fluorite K⁰_{sp} (a_{Ca²⁺}a²_{F⁻}) derived from our measurements in pure water is 3.07 ± 0.09 * 10⁻¹¹ whereas the average value for the pure water, NaCl and Na-Cl-Ca solutions combined is 3.08 ± 0.08 * 10⁻¹¹.

Experiments run in Na-Cl-Ca-Mg and artificial seawater solutions failed to reproduce the K⁰_{sp} obtained in pure water and the simple salt solutions. Part of this discrepancy could be attributed to the inaccuracy of activity coefficient estimates obtained from speciation models, but we believe that they result from the formation of Mg bearing CaF₂ solid solutions on the surface of fluorite. Since the equilibrium ion activity product is more than one order of magnitude larger in the Na-Cl-Ca-Mg solution than in artificial seawater we can only assume that other seawater constituents affect the composition of the solubility-controlling phase, possibly Sr²⁺, CO₃²⁻ and boric acid.

3.2 Introduction

Fluorite is by far the most important fluorine bearing mineral phase in Earth's crust and is thought to control the fluoride (F⁻) concentration in seawater and other natural aqueous solutions (Nordstrom and Jenne, 1977; Elrashidi and Lindsay, 1986). The fluoride ion, one of the major, conservative seawater constituents (F⁻/Cl = 6.75 ± 0.03 * 10⁻⁵ g_i/Cl; Warner, 1971) has a concentration of 6.8 * 10⁻⁵ M in S=35 seawater.

The solubility of fluorite can be described by the following reaction:



The thermodynamic equilibrium constant for this reaction is expressed in terms of the activities of the products and reactants according to the following:

$$K_{\text{sp}}^0 = \frac{a_{\text{Ca}^{2+}} a_{\text{F}^{-}}^2}{a_{\text{CaF}_2}} \quad (3.2)$$

where K_{sp}^0 is the equilibrium thermodynamic solubility product and a is the equilibrium activity of the ion. If the solid is pure, its activity is, by definition, unity, and equation 3.2 reduces to:

$$K_{\text{sp}}^0 = [\text{Ca}^{2+}](\gamma_{\text{Ca}^{2+}})[\text{F}^{-}]^2(\gamma_{\text{F}^{-}})^2 = K_{\text{sp}}^*(\gamma_{\text{Ca}^{2+}})(\gamma_{\text{F}^{-}})^2 \quad (3.3)$$

where K_{sp}^* is the stoichiometric solubility product; γ are the total ion activity coefficients; $[i]$ are the equilibrium total ion molal concentrations.

Table 3.0 is a compilation of the thermodynamic solubility constant values at 25⁰C and 1 atmosphere total pressure taken from the literature. The values vary by nearly one order of magnitude and highlight the need for further refinement.

Table 3.0 Compilation of fluorite K_{sp}^0 values reported in the literature.

K_{sp}^0	Source
$5.88 * 10^{-12}$	Strubel (1965)
$8.15 * 10^{-12}$	Naumov et al. (1971)
$1.10 * 10^{-11}$	Nordstrom & Jenne (1977)
$2.51 * 10^{-11}$	Nordstrom et al. (1990)
$2.69 * 10^{-11}$	Smyshlyaev & Edeleva (1962)
$2.70 * 10^{-11}$	Sadiq & Lindsay (1979)
$3.12 * 10^{-11}$	Robie et al. (1978)
$3.89 * 10^{-11}$	Elrashidi & Lindsay (1986)
$3.98 * 10^{-11}$	Wagman et al. (1981)

The stoichiometric solubility of fluorite in seawater has never been experimentally determined. It could be calculated from the K_{sp}^0 and estimates of the Ca^{2+} and F^- activity coefficients in seawater (see Equation 3.3). The estimated activity coefficient of Ca^{2+} in seawater is fairly well constrained by experimental measurements of the stoichiometric solubility of calcite and aragonite in seawater (0.203; Mucci, 1983). The activity coefficient of F^- (γ_{F^-}) in seawater was derived experimentally from measurements of the apparent dissociation constant of HF in a water-NaCl-Na₂SO₄-MgCl₂-CaCl₂-HCl solution at an ionic strength corresponding to $S=34.6$ (0.296; Culberson et al., 1970). As a first approximation this method appears to provide a reasonable value but two reasons warrant further investigation. The experimental solution was not seawater, and the apparent dissociation of HF, occurs in the 3-4 pH range, conditions which are not truly representative of natural seawater.

In this study, fluorite equilibration experiments were carried out in a variety of aqueous solutions at 25⁰C and 1 atmosphere total pressure to determine the effect of ionic strength and the potential co-precipitation of seawater constituents on the solubility of fluorite. The stoichiometric solubility constant of fluorite was measured in pure water,

0.1, 0.4 and 0.7 molar NaCl solutions as well as in 10 mM CaCl₂ + 0.64 M NaCl (Na-Cl-Ca solution), 10 mM CaCl₂ + 0.484 M NaCl + 52 mM MgCl₂ (Na-Cl-Ca-Mg solution), and artificial seawater. In the latter three solutions, equilibrium was approached from both undersaturation (i.e., initial [F⁻] = 0) and supersaturation (i.e., initial [F⁻] = 15 times the seawater value \cong 1 mM) to test for reversibility and confirm equilibrium.

Measurements were carried out at pH \leq 7.5 and P_{CO₂} = atmospheric, thus, all the solutions are undersaturated with respect to calcite (Mucci, 1983).

3.3 Materials & Methods

Chemicals used for all experiments and analytical procedures were reagent grade or better. Specific grades were used as required by some techniques and described thoroughly in the relevant sections. All glassware and reusable plasticware were rinsed with Nanopure™ water after soaking in a 10% nitric (glassware) or 10% HCl (Plasticware) acid bath for at least 12 hours. Millipore Nanopure™ water was used for preparation of all solutions except where indicated.

Fisher Scientific C-89 certified calcium fluoride (CaF₂) powder was used for the solubility measurements. The fluorite was cleaned by multiple rinsing with Nanopure™ water and subsequently oven-dried at 110° C for a period of 24 hours. The fluorite is a fine white powder with an average grain size of 20 ± 5 microns as determined by field-emission gun scanning electron microscopy (FEG-SEM). Its X-ray diffraction pattern is a perfect match to the JCPDS reference pattern 35-0816. X-ray fluorescence analysis of the powder, using a Philips PW2400 3kW automated XRF spectrometer system with a Rhodium 60 kV end window x-ray tube (Table 3.1) revealed that the fluorite is pure with very little impurities.

Table 3.1 Fluorite major and trace element composition (XRF)

SiO ₂	0.05%	CaO	69.51%	Cr ₂ O ₃	<d/l
TiO ₂	0.009%	Na ₂ O	0.17%	V	< d/l
Al ₂ O ₃	0.06%	K ₂ O	< d/l	Zn	< d/l
Fe ₂ O ₃	0.03%	P ₂ O ₅	0.009%	LOI	30.14%
MnO	< d/l	BaO	< d/l		

d/l: Detection limit is 1 ppm

Artificial seawater was prepared in 10 kg batches with distilled water according to the recipe of Kester et al. (1969) except that NaHCO_3 was added as required to adjust the pH to about 7.0 on the total hydrogen concentration scale.

Concentrated stock solutions of the hydrated salts (i.e., MgCl_2 , CaCl_2 and SrCl_2) were titrated against a silver nitrate solution, itself standardized against a solution prepared gravimetrically from NaCl salt dried at 110°C for at least 24 hours and stored in a vacuum dessicator. The salinity of all the artificial seawater solutions used throughout this study was 35.0 ± 0.5 as determined by titration with a silver nitrate solution standardized against IASPO standard seawater. The reproducibility of these titrations was better than $\pm 0.5\%$.

Solutions of 0.1, 0.4 and 0.7 M NaCl were prepared gravimetrically from NaCl salt dried at 110°C for at least 24 hours and stored in a vacuum dessicator. Solutions of 10 mM CaCl_2 , mixed 10 mM CaCl_2 + 0.64 M NaCl and mixed 10 mM CaCl_2 + 0.484 M NaCl + 52 mM MgCl_2 were prepared as described above.

The pH of each solution was measured with an Ag/AgCl ORION combination electrode using a Radiometer Copenhagen PHM 84 Research pH meter. The electrode was calibrated using three NIST-traceable buffers at pH 4.00, 7.00 and 10.00. The pH of a TRIS buffer solution prepared in artificial seawater or TRIS buffer in > 0.1 M NaCl solutions (Millero et al., 1987; 1993) was used in order to convert all measurements to the total hydrogen concentration scale.

One hundred and fifty to 200 milligrams of fluorite powder were transferred to 60 ml high density polyethylene Nalgene™ bottles. The bottles were then filled with the experimental solutions to the bottleneck and sealed with screwcaps. The bottles were

mounted on a rotating table (5 rpm) immersed in a constant temperature bath (Mucci, 1983) and maintained at $25 \pm 0.5^\circ\text{C}$.

The solutions were equilibrated with fluorite for periods ranging from 4 to 64 weeks. Prior to sampling, the bottles were removed from the rotating table and allowed to sit upright so the fluorite could settle before they were uncapped and the pH measured. An ORION combination electrode, fitted with a piece of Tygon™ tubing and Parafilm™ to form an airtight seal, was immediately inserted in the neck of the bottle. After the pH measurements, the solution was drawn from the bottle using a 60 ml plastic syringe, filtered through a $0.45\ \mu\text{m}$ HA Millipore filter and transferred to a clean 60 ml high density polyethylene Nalgene bottle.

Calcium concentrations in the 10 mM CaCl_2 + 0.64 M NaCl, 10 mM CaCl_2 + 0.484 M NaCl + 52 mM MgCl_2 , and artificial seawater solutions were determined potentiometrically with EGTA using the method described by Lebel and Poisson (1976). The titrant was standardized with IASPO standard seawater. The reproducibility of these titrations was better than $\pm 0.5\%$. Calcium concentrations in pure water and the NaCl solutions were determined by flame atomic absorption spectroscopy (FAAS) using a Perkin Elmer 3100. External standards prepared from a 1000 ppm (Fisher Scientific # CSC191-500) Ca standard stock solution was matrix-matched and analyzed to construct a calibration curve. The detection limit for Ca using this method is 0.08 ppm ($2.0\ \mu\text{mol/l}$) and the RSD on three replicate measurements was below 5%.

The lanthanum (III)/Alizarin Fluorine Blue spectrophotometric method of Hanocq and Molle (1968) was used to measure fluoride concentrations. Absorbance measurements were performed on a Hewlett Packard 8453 UV-Visible

spectrophotometer using a 10 mm quartz cuvette. The detection limit and linear range of this method are reported as 0.075 ppm (3.95 $\mu\text{mol/L}$) and 0.075 ppm (3.95 $\mu\text{mol/L}$) to 1.2 ppm (63.2 Mmol/l) respectively. Calibrations were conducted for each analytical session using solutions diluted from a gravimetrically prepared 1000 ppm NaF stock solution. Standards were analyzed in triplicate and corrections for blanks were applied. R^2 values of the calibration curves were always above 0.995. Samples were measured in triplicate and RSD% values were generally under 5%. Calibration standards and samples were matrix-matched.

3.4 Results and Discussion

Results of the equilibrations in all experimental solutions are assembled in Appendix 3.7.1 and 3.7.2. In all cases, the ion concentration products ($ICP = [Ca^{2+}][F^{-}]^2$) measured after 32 weeks of equilibration become invariant or converge to constant values (e.g., see Figure 3.0).

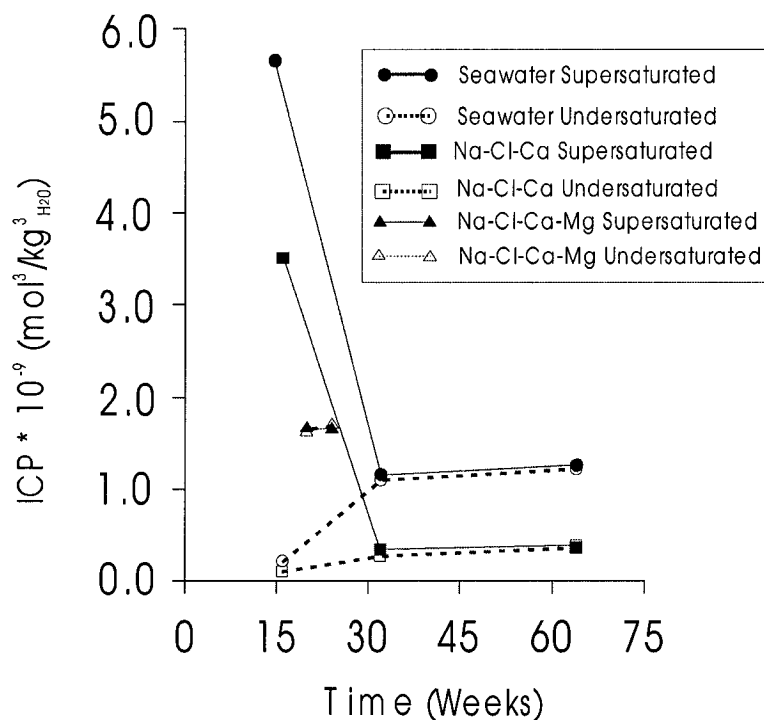


Figure 3.0 Measured ion concentration products (ICP) for the Na-Cl-Ca, Na-Cl-Ca-Mg and seawater solutions as a function of the period of equilibration.

Convergence of the ICP values from the undersaturated and supersaturated Na-Cl-Ca, Na-Cl-Ca-Mg, and artificial seawater solutions confirms that equilibrium was reached and the reaction is reversible. Average values of pH and ICP for each solution measured after 32 weeks of equilibration (after 20 weeks for the Na-Cl-Ca-Mg solutions) are reported in Table 3.2 and, thus, represent equilibrium values or K_{sp}^* .

Table 3.2 Results of the 32 and 64-week pure water, NaCl, Na-Cl-Ca and seawater solution sample analyses and the 20 and 24 week Na-Cl-Ca-Mg solution sample analyses. Activity coefficients were obtained with the PHREEQC v.2 computer code (Parkhurst and Appelo, 1999).

Solution	# samplings	equilibration period (weeks)	pH _{total H scale}	[Ca ²⁺][F ⁻] ²	$\gamma_{Ca^{2+}}$	γ_{F^-}	$a_{Ca^{2+}} a_{F^-}^*$
Nanopure™	2	32 & 64	7.61 ± 0.12	3.67 * 10 ⁻¹¹	0.887	0.971	3.07 * 10 ⁻¹¹
0.1 M NaCl	2	32 & 64	7.59 ± 0.14	1.35 * 10 ⁻¹⁰	0.390	0.760	3.04 * 10 ⁻¹¹
0.4 M NaCl	2	32 & 64	7.54 ± 0.04	2.68 * 10 ⁻¹⁰	0.270	0.649	3.05 * 10 ⁻¹¹
0.7 M NaCl	2	32 & 64	7.70 ± 0.22	3.55 * 10 ⁻¹⁰	0.249	0.603	3.21 * 10 ⁻¹¹
10 mM CaCl ₂ + 0.64 M NaCl	2 und & 2 sup	32 & 64	7.37 ± 0.06	3.26 * 10 ⁻¹⁰	0.250	0.607	3.00 * 10 ⁻¹¹
10 mM CaCl ₂ + 52 mM MgCl ₂ + 0.484 M NaCl	2 und & 2 sup	20 & 24	7.57 ± 0.19	1.68 * 10 ⁻⁹	0.252	0.615	1.60 * 10 ⁻¹⁰
Seawater	2 und & 2 sup	32 & 64	7.51 ± 0.06	1.15 * 10 ⁻⁹	0.249	0.606	1.05 * 10 ⁻¹⁰
				†	0.203	0.296	2.04 * 10 ⁻¹¹
				‡	0.203	0.333	2.58 * 10 ⁻¹¹
				±	0.203	0.309	2.23 * 10 ⁻¹¹

* Please note that concentrations were converted to molal units since activity coefficient estimates are in molal⁻¹. † $\gamma_{Ca^{2+}}$ (Mucci, 1983), γ_{F^-} (Culberson et al. 1970), • γ_{F^-} (Millero & Schreiber, 1982), ‡ γ_{F^-} (Millero & Pierrot, 1998)

Fluorite stoichiometric solubility products (K^*_{sp}) measured in pure water and NaCl solutions are plotted as a function of ionic strength in Figure 3.1.

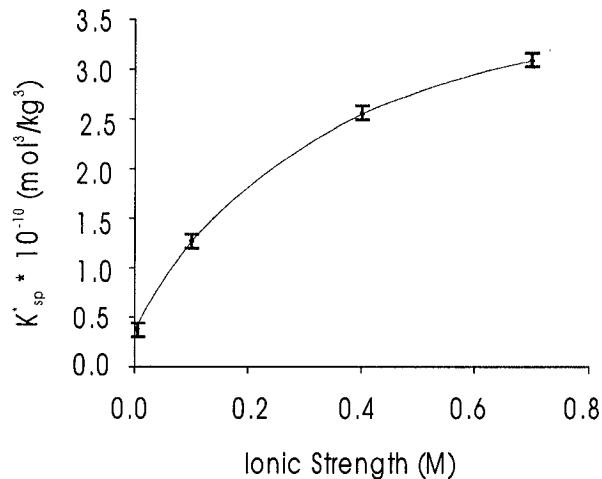


Figure 3.1 The stoichiometric solubility constant of fluorite in NaCl solutions of various ionic strengths at 25°C and 1 atmosphere total pressure. Error bars correspond to 2σ of the average of the 32 and 64 week ICP's.

As expected, an increase in ionic strength translates into an increase in $K_{\text{CaF}_2}^*$ as the ion activity coefficients of Ca^{2+} and F^- decrease over the range of ionic strengths investigated.

The fluorite K_{sp}^0 ($a_{\text{Ca}^{2+}} a_{\text{F}^-}^2$) derived from the measured K_{sp}^* and ion activity coefficient estimates obtained using PHREEQC v 2.0 (Parkhurst and Appelo, 1999) for pure water is $3.07 \pm 0.09 * 10^{-11}$ whereas the average value for the pure water, NaCl and Na-Cl-Ca solutions combined is $3.08 \pm 0.08 * 10^{-11}$. The K_{sp}^0 value determined in these solutions is identical to the value $3.12 * 10^{-11}$ reported in Robie et al. (1978).

On the other hand, the equilibrium CaF_2 IAP's derived for the Na-Cl-Ca-Mg and artificial seawater solutions are significantly higher than the K_{sp}^0 (Table 3.2). A number of explanations are possible for these discrepancies. The speciation model PHREEQC v 2.0 (Parkhurst and Appelo, 1999) may not provide accurate estimates of the activity coefficients of the Ca^{2+} and F^- ions in these solutions. This is unlikely for the Na-Cl-Ca-Mg solution since it provides estimates in the Na-Cl-Ca solutions that yield very consistent K_{sp}^0 values. Furthermore, the activity coefficients of the Ca^{2+} and F^- ions (0.262. and 0.598, respectively) generated by a Pitzer model Excel™ macro provided by Millero (pers. comm., 2002) for the Na-Cl-Ca-Mg solution are nearly identical to those estimated by the PHREEQC computer code (0.252 and 0.615, respectively; Table 3.2).

The activity coefficients estimated for the seawater solution by the PHREEQC computer code (i.e., $\gamma_{\text{Ca}^{2+}} = 0.249$ & $\gamma_{\text{F}^-} = 0.606$), are different, especially for F^- , than those obtained using the ion pairing model of Millero and Schreiber (1982) ($\gamma_{\text{F}^-} = 0.333$), the specific interaction model of Millero & Pierrot (1998) ($\gamma_{\text{F}^-} = 0.309$) as well as the experimentally derived value of Culberson et al. (1970) ($\gamma_{\text{F}^-} = 0.296$). The equilibrium

IAP obtained for seawater using activity coefficients generated by the PHREEQC computer code is $1.05 * 10^{-10}$ compared to $2.58 * 10^{-11}$ ($\gamma_{F^-} = 0.333$), $2.23 * 10^{-11}$ ($\gamma_{F^-} = 0.309$) and $2.04 * 10^{-11}$ ($\gamma_{F^-} = 0.296$) obtained by using $\gamma_{Ca^{2+}} = 0.203$, derived from the $CaCO_3$ solubility measurements of Mucci (1983), and the γ_{F^-} values obtained from the literature listed above. Whichever value of γ_{F^-} is used, the equilibrium IAP is different than the K_{sp}^0 obtained in this study for pure water and Na-Cl-Ca solutions (Table 3.2) and, thus, casts a doubt on the validity of γ_{F^-} estimates. Based on our measurement of the equilibrium ICP of fluorite in seawater, the K_{sp}^0 of fluorite determined in this study and reported by Robie et al. (1978), and $(\gamma_{Ca^{2+}})_{sw}$ derived by Mucci (1983), we estimate γ_{F^-} at 0.366 in seawater (equation 3.4).

$$\gamma_{F^-} = \sqrt{\frac{K_{sp}^0}{K_{sp}^* \gamma_{Ca^{2+}}}} \quad (3.4)$$

Alternatively, it may be that the solubility-controlling phase in these solutions is not pure fluorite but a solid solution of yet undetermined composition. In the Na-Cl-Ca-Mg solution, this phase would have to be a mixed Ca-Mg fluoride whose solubility is greater than pure fluorite. Sellaite, a mineral with the formula MgF_2 has a $K_{sp}^0 = 9.77 * 10^{-9}$ (Elrashidi and Lindsay, 1986). Given that the solubility of sellaite is greater than that of fluorite, an ideal solid solution of composition $Ca_xMg_{(x-1)}F_2$ would, according to equation 3.5, where χ is the mole fraction of CaF_2 in the solid solution and () are the ion activities,

$$IAP = \frac{(Ca^{2+})(F^-)^2}{\chi_{CaF_2}} \quad (3.5)$$

have a K_{sp}^0 greater than fluorite and could account for the high IAP measured in this solution. Such solid solutions are not documented in the literature but Appollonov (1966) reports on a hydrothermal fluorite deposit in central Russia which includes zones of fluorite-sellaite aggregates and suggested that these formed from the decomposition of the metastable phase $4CaF_2 \cdot 3MgF_2$.

A solid-solution of yet undetermined composition may also account for the IAP- K_{sp}^0 discrepancy in the seawater solution. Its composition may as well contain Mg but the incorporation of Sr may also play a critical role. Strontium is reported to often substitute for calcium in the fluorite lattice. Both Deer et al. (1992) and Eppinger and Closs (1990) report that some fluorites are particularly rich in strontium, containing up to 1 % Sr. Unlike Mg (MgF_2) there is no mention in the literature of a mineral of the formula SrF_2 but the natural occurrence of BaF_2 (Frankdicksonite; Radtke and Brown, 1974) with the fluorite structure certainly implies the existence of natural SrF_2 and the possible existence of $Ca_xSr_{(x-1)}F_2$ solid-solutions.

Other major seawater constituents may interact with the fluorite crystal and alter its solubility, including boric acid/borate and the carbonate ion. Nordstrom and Jenne (1977) report that F^- and borate ($B(OH)_4^-$), present at their respective seawater concentrations, form strong complexes and possibly these may develop on the crystal lattice. The interaction between Ca^{2+} and the carbonate ion (CO_3^{2-}) is strong and calcite may crystallize on the fluorite lattice. Both processes would alter the solubility of fluorite.

3.5 Conclusion

The goal of this study was to accurately determine the activity coefficient of the fluoride ion in seawater and was to be achieved by measurements of the stoichiometric solubility of fluorite at 25⁰C and 1 atmosphere total pressure. Results of similar measurements in pure water and simple salt solutions when coupled to estimates of the activity coefficients of F⁻ and Ca²⁺ generated by the PHREEQC computer code (Parkhurst and Appelo, 1999) produced an average K_{sp}⁰ of $3.06 \pm 0.08 * 10^{-11}$, a value indistinguishable from the value of $3.12 * 10^{-11}$ derived from the thermodynamic database found in Robie et al. (1976).

Experiments run in Na-Ca-Mg-Cl and artificial seawater solutions at I = 0.7 M failed to replicate the K_{sp}⁰ obtained in the pure water and the simple salt solutions. Whereas part of this discrepancy could be attributed to the inaccuracy of activity coefficient estimates obtained from speciation models, we believe that they result from the formation of solubility-controlling Mg-bearing CaF₂ solid solutions on the surface of the fluorite seed mineral. Since the equilibrium ion activity product in the presence of fluorite is more than one order of magnitude larger in the Na-Cl-Ca-Mg solution than in artificial seawater we can only assume that other seawater constituents affect the composition of the solubility-controlling phase, possibly Sr²⁺, CO₃²⁻ and boric acid.

3.6 References

- Apollonov, V.N., 1966. Discovery of sellaite in Uzbekistan. *Uzb. Geol. Zh.*, 10: 10-15. (in Russian, with English Abstr.)
- Culberson, C., Pytkowicz, R.M., Hawley, J.E., 1970. Seawater alkalinity determination by the pH method. *J. Mar. Res.*, 28: 15-21.
- Deer, W.A., Howie, R.A. and Zussman, J., 1992. *Rock Forming Minerals*, 2nd ed. William Clowes and Sons, London.
- Eppinger, R.G., Closs, L.G., 1990. Variation of trace elements and rare earth elements in fluorite: A possible tool for exploration. *Econ. Geol.*, 85: 1896-1807.
- Elrashidi, M.A., Lindsay, W.L., 1986. Chemical equilibria of fluorine in soils: A theoretical development. *Soil Sci.*, 141: 275-280.
- Hanocq, M., Molle, L., 1968. Dosage par spectrophotométrie dans l'ultraviolet de l'ion fluorure a l'aide des chélates. *Analytica Chimica Acta.*, 42: 349-356.
- Kester D. R., Duedall I. W., Connor D. N., Pytkowicz R. M., 1969. Preparation of artificial seawater. *Limnol. Oceanog.*, 12: 176-179.
- Lebel, J., Poisson, A., 1976. Potentiometric determination of calcium and magnesium in seawater. *Mar. Chem.*, 4: 321-332.
- Millero, F.J., Schreiber, D.R., 1982. Use of the ion pairing model to estimate activity coefficients of the ionic components of natural waters. *Amer. J. Sci.*, 282: 1508-1540.
- Millero, F.J., Hershey, J.P., Fernandez, M., 1987. The pK^* of TRISH⁻ in Na-K-Mg-Ca-Cl-SO₄ brines -pH scales. *Geochim. Cosmochim. Acta*, 51: 707-711.
- Millero, F.J., Zhang, J.Z., Fiol, S., Sotolongo, S., Roy, R.N., Lee, K., Mane, S., 1993. The use of buffers to measure the pH of seawater. *Mar. Chem.*, 44: 143-152.
- Millero, F.J., Pierrot, D., 1998. A chemical equilibrium model for natural waters. *Aquatic Geochemistry* 4: 153-199.
- Mucci, A., 1983. The solubility of calcite and aragonite in seawater at various salinities, temperatures, and one atmosphere total pressure. *Amer. J. Sci.*, 283: 780-799.
- Naumov, G.B., Rhyzenko, B.N., Khodakovskiy, I.L., 1971. *Handbook of Thermodynamic Data*. Natl. Tech. Infor. Serv. Rep. PB-226 722. U.S. Dept. Comm.
- Nordstrom, D.K., Jenne, A.J., 1977. Fluorite solubility equilibria in selected geothermal waters. *Geochim. Cosmochim. Acta*, 41: 175-188.

Nordstrom, D.K., Plummer, L.N., Langmuir, D., Busenberg, E., May, H.M., Jones, B.F., Parkhurst, D.L., 1990. Revised chemical equilibria data for major water-mineral reactions and their limitations. In: D.C. Melchior and R.L. Basset (Editors), *Chemical Modeling of Aqueous Systems II*. American Chemical Society, Washington D.C., pp. 398-413.

Parkhurst, D.L., Appelo, C.A.J., 1999. User's guide to PHREEQC (version 2). A computer program for speciation, batch-reaction, one-dimensional transport, and inverse geochemical calculations. U.S. Geological Survey Water-Resources Investigations Report 99-4259.

Radtke, A.S., Brown, G.E., 1974. Frankdicksonite, BaF_2 , a new mineral from Nevada. *Am. Mineral.*, 59: 9-10.

Robie, R.A., Hemingway, B.S., Fisher, J.R., 1978. Thermodynamic properties of Minerals and related substances at 298.15 K and 1 bar pressure and at higher temperatures. *Geol. Surv. Bull.*, 1452, U.S. Government printing office, Washington D.C.

Sadiq, M., Lindsay, W.L., 1979. Selection of standard free energies of formation for use in soil chemistry. *Colorado State Univ. Exp. Sta. Tech. Bull.* 134.

Smyshlyaev, S.I., Edelva, N.P., 1962. Determination of solubility of minerals. I. The solubility product of fluorite. *Izv. Vysshikh Uchebn. Zavedenii Khim. Teknol.*, 5: 871.

Strübel, G., 1965. Quantitative untersuchungen über die hydrothermale löslichkeit von flusspat (CaF_2). *Neues Jahrb. Mineral. Monatsh.*, 3: 83-95.

Wagman, D.D., Evans, W.H., Parker, V.B., Schumms, R.H., Nuttall, R.L., 1981. Selected values of chemical thermodynamic properties. *Nat. Bur. Sd. Tech. Note* 270-8.

Warner, T.B., 1971. Normal fluoride content of seawater. *Deep-Sea Res.*, 18: 1255-1263.

3.7 Appendix

Appendix 3.7.1 Fluorite solubility data in pure water and NaCl solutions.

Solution	Sampling	pH _{tot H scale}	[Ca ²⁺] _{molal} (± 0.5%)	[F ⁻] _{molal} (± 5.0%)
Nanopure™ Water	8 weeks	7.55	2.84E-04	3.7E-04
	16 weeks	7.47	2.69E-04	3.9E-04
	32 weeks	7.66	2.87E-04	3.6E-04
	64 weeks	7.70	2.76E-04	3.6E-04
0.1 M NaCl	8 weeks	7.58	4.53E-04	6.1E-04
	16 weeks	7.46	4.50E-04	6.2E-04
	32 weeks	7.60	4.12E-04	5.6E-04
	64 weeks	7.53	4.20E-04	5.8E-04
0.4 M NaCl	8 weeks	7.51	5.50E-04	7.6E-04
	16 weeks	7.46	5.60E-04	8.0E-04
	32 weeks	7.40	5.11E-04	7.3E-04
	64 weeks	7.48	5.12E-04	7.1E-04
0.7 M NaCl	8 weeks	7.76	5.42E-04	8.6E-04
	16 weeks	7.68	5.51E-04	8.9E-04
	32 weeks	7.72	5.10E-04	8.3E-04
	64 weeks	7.78	5.03E-04	8.5E-04

Appendix 3.7.2 Fluorite solubility data in mixed salt and artificial seawater solutions from both undersaturation and supersaturation

Solution	Sampling	pH _{tot H calc}	[Ca ²⁺] _{molal} (± .5%)	[F ⁻] _{molal} (± 5.0%)
10 mM CaCl ₂ + 0.64 M NaCl				
Undersaturated	8 weeks	7.25	9.84E-03	9.2E-05
	16 weeks	7.35	9.72E-03	9.7E-05
	32 weeks	7.30	9.84E-03	1.8E-04
	64 weeks	7.43	9.77E-03	1.9E-04
10 mM CaCl ₂ + 0.64 M NaCl				
Supersaturated	16 weeks	7.38	9.17E-03	6.2E-04
	32 weeks	7.30	9.31E-03	1.9E-04
	64 weeks	7.45	9.05E-03	1.9E-04
Artificial Seawater				
Undersaturated	8 weeks	7.35	1.10E-02	9.4E-05
	16 weeks	7.53	1.07E-02	1.1E-04
	32 weeks	7.50	1.08E-02	3.2E-04
	64 weeks	7.49	1.06E-02	3.4E-04
Artificial Seawater				
Supersaturated	16 weeks	7.60	1.05E-02	7.4E-04
	32 weeks	7.46	1.05E-02	3.3E-04
	64 weeks	7.46	1.04E-02	3.4E-04
0.484 M NaCl + 10 mM CaCl ₂ + 52 mM MgCl ₂				
Undersaturated	20 weeks	7.88	1.12E-02	3.8E-04
	24 weeks	7.63	1.09E-02	4.0E-04
0.484 M NaCl + 10 mM CaCl ₂ + 52 mM MgCl ₂				
Supersaturated	20 weeks	7.75	1.07E-02	3.9E-04
	24 weeks	7.65	1.04E-02	4.1E-04

CHAPTER 4

Conclusion

Contribution to Knowledge

This study is one of few to describe the adsorption behavior of arsenate and phosphate on gibbsite from a variety of solutions, including seawater, at realistic natural adsorbate concentrations. Adsorption of phosphate and arsenate onto gibbsite in the absence of the fluoride ion is greatest in pure water and least in 0.67 M NaCl. This implies that adsorption of both oxyanions on gibbsite is either not purely inner-sphere or the formation of ion pairs with the background electrolyte, Na, stabilizes the adsorbates in solution. The presence of Ca at its seawater concentration partially counteracts the decrease in adsorption of both adsorbates caused by the increase in ionic strength. The formation of adsorbate/Ca aqueous complexes that have a strong affinity for, and form ternary complexes, with the gibbsite surface are thought to be responsible for the increased adsorption.

For the first time, arsenate and phosphate are observed to behave very differently with respect to their respective adsorption onto gibbsite. In the presence of an inexhaustible amount of fluoride at near seawater concentration, arsenate is adsorbed onto gibbsite in significantly greater amounts than phosphate, irrespective of solution composition (i.e., pure water, NaCl solution, seawater etc...). The formation of arsenate-fluoride aqueous complexes and their adsorption to the gibbsite surface as ternary surface complexes may account for the significant increase in adsorption in the presence of fluoride ions. The absence of a similar behavior with phosphate may reflect a lack of affinity or availability of the phosphate-fluoride complexes.

These results have interesting implications with respect to the fate of arsenate and phosphate during estuarine mixing. The increase in ionic strength experienced by a

gibbsite particle as it is carried by river waters through an estuary will induce desorption of both arsenate and phosphate. At the same time, the concentration of Ca^{2+} (i.e., $[\text{Ca}^{2+}]_{\text{RW}} = 0.74 \text{ mM}$, $[\text{Ca}^{2+}]_{\text{SW}} = 10.28 \text{ mM @ } S = 35$) will increase and partially counteract the effect of the increasing ionic strength. Finally, a concurrent increase of the concentration of F^- (i.e., $[\text{F}^-]_{\text{RW}} = 5.0 \mu\text{M}$, $[\text{F}^-] = 70.0 \mu\text{M @ } S = 35$) will promote arsenate adsorption but inhibit phosphate adsorption. The combination of factors will likely result in some desorption of phosphate and very little desorption of arsenate. It is also possible that the release of some phosphate will liberate adsorption sites to be occupied by arsenate.

We chose the mineral fluorite to buffer some of the experimental solutions with respect to the fluoride ion activity and searched the literature to find its stoichiometric solubility (K_{sp}^*) in seawater and, hence, derive the equilibrium fluoride concentration in this solution and discovered that it has never been measured. Alternatively, it could be derived from the thermodynamic solubility constant (K_{sp}^0) of fluorite and the activity coefficients of the calcium and fluoride ions in the various experimental solutions including seawater but the values of K_{sp}^0 found in the literature vary by one order of magnitude and highlight the need for further refinement.

Our fluorite equilibration experiments yielded a $K_{\text{sp}}^0 (a_{\text{Ca}^{2+}} a_{\text{F}^-}^2)$ in pure water of $3.07 \pm 0.09 * 10^{-11}$ whereas the average value for the Nanopure™ water, NaCl and Na-Cl-Ca solutions combined is $3.08 \pm 0.08 * 10^{-11}$. The solubility constant measured in these solutions is identical to the value (i.e., $3.12 * 10^{-11}$) reported in Robie et al. (1978). On the other hand, the equilibrium IAP's in the Na-Cl-Ca-Mg and artificial seawater solutions are significantly higher than the K_{sp}^0 . Whereas part of this discrepancy could be

attributed to the inaccuracy of activity coefficient estimates obtained from speciation models, it is likely the result of the formation of solubility-controlling, Mg-bearing, CaF_2 solid solutions on the surface of fluorite. Since the equilibrium ion activity product in the presence of fluorite is more than one order of magnitude larger in the Na-Cl-Ca-Mg solution than in artificial seawater, we can only assume that other seawater constituents affect the composition of the solubility-controlling phase, possibly Sr^{2+} , CO_3^{2-} and boric acid.

Suggestions for Future Research

In this thesis, adsorption of phosphate and arsenate onto gibbsite was studied at the macroscopic scale and quantified by simple empirical theories. To fully explore the relationship between arsenate and phosphate, and the gibbsite surface during estuarine mixing, the full development of a surface complexation model is required. Such an undertaking would require several key assessments such as; the adsorption of all major seawater ions to gibbsite in an indifferent electrolyte at the ionic strength of seawater; the measurement of the surface acidity constants of gibbsite in single major seawater ion solutions and in seawater; speciation of arsenate and phosphate in seawater; and the adsorption of arsenate and phosphate in seawater. It would also be necessary to carry out adsorption studies over the range of pH's encountered in estuarine settings and, in turn, would require a series of indifferent seawater buffers to control the pH. Only then can the use of a model (e.g., constant capacitance model Hohl & Stumm (1976); triple layer model Stern (1924); multi-site complexation models Hiemstra et al., (1989)) be tested against experimental data and, hence, provide a predictive tool for natural settings.

With the development of techniques such as extended x-ray absorption fine structure spectroscopy (EXAFS), the actual nature of the surface complexes can be determined. Using such a technique would confirm or infirm the existence of Ca-phosphate/arsenate and F-arsenate ternary surface complexes, and would certainly reveal other configurations.

In terms of our experimental protocol, some changes in the methods would provide a more complete set of data. The accuracy of arsenic measurements could be improved by a different analytical method, which covers the concentration range

investigated in this study, without a dilution step. Given the nutrient status of phosphorus and the low concentrations investigated, sterilization of the reactional system would certainly eliminate the potential role of bacterial uptake. Quantifying the role of organic matter with respect to arsenate and phosphate adsorption on gibbsite in the experimental solutions would provide a much more realistic simulation of the natural environment.

With respect to the fluorite equilibration experiments, in particular, in the Na-Cl-Ca-Mg and artificial seawater solutions, running experiments in large volumes of solutions and continually re-supplying the solution with fluoride in order to grow these solid:solutions may provide enough sample for chemical and mineralogical determination. Similarly, initiating similar experiments in a simple NaCl solution and progressively building up to seawater composition, and continually analyzing the solid fraction, may isolate the role and composition of co-precipitates.